The University of British Columbia

Faculty of Graduate Studies

PROGRAMME OF THE

FINAL ORAL EXAMINATION

FOR THE DEGREE OF

DOCTOR OF PHILOSOPHY

of

C. DONALD COX

B. Sc., University of New Brunswick
M. Sc., McMaster University

IN ROOM 301 PHYSICS BUILDING

MONDAY, JUNE 15th, 1959 at 3:00 P. M.

COMMITTEE IN CHARGE

DEAN G. M. SHRUM: Chairman

R. E. BURGESS	M. F. McGREGOR
G. M. GRIFFITHS	E. V. BOHN
J. B. BROWN	F. NOAKES
A. M. CROOKER	J. B. GUNN

External Examiner: H. Y. FAN
Purdue University

BULK PHOTO-EFFECTS IN INHOMOGENEOUS SEMICONDUCTORS

ABSTRACT

An observable e. m. f. exists in a semiconductor when a non-equilibrium carrier concentration is present in a region of electrostatic potential gradient. These two conditions may arise in a variety of ways, and the e. m. f. 's associated with various combinations of conditions are listed. One of these e. m. f. 's arises from a photo-generated non-equilibrium carrier concentration in regions of electrostatic potential gradient due to an inhomogeneous impurity distribution. The thesis is chiefly concerned with the extention of the theory of this bulk photo e. m. f. and its comparison with experiment.

Previous work on the subject is reviewed and the theory is developed to cover all conditions of illumination in the region of an arbitrary impurity density gradient. An expression for the bulk photo e. m. f. is derived by two approaches, integration of the electrostatic potential gradient, and integration of the carrier quasi Fermi levels, over the illuminated region. The latter derivation is shown to be more general in its application, and is used to obtain an expression for the photo e. m. f. both in an illuminated p-n junction and in an illuminated bulk inhomogeneity. Using the general result, expressions for the e. m. f. are written for the extreme cases of weak and strong illumination in extrinsic and nearly intrinsic semiconductors. The relation between bulk photo e. m. f. and photoconductive resistance decrease is examined.

Measurements were made of the bulk photo e. m. f. as a function of light intensity. The proportionality of the effect at low levels of illumination was verified. Observations of the photo e. m. f. patterns showed a maximum of e. m. f. at positions of maximum conductivity gradient. Since the bulk photo e. m. f. is a function of conductivity gradient, light probe measurements give a sensitive technique for the detection of inhomogeneous impurity distributions. With

weak illumination, the measured ratio of photo e. m. f. to photoconductive resistance decrease was a constant independent of light intensity. These observations verified the theory and suggested a use for this ratio in quantitative measurements of conductivity gradient. The photo e. m. f. at strong illumination was shown to be dependent on the impurity distribution outside the region of incident light. The conditions under which the ratio of photo e. m. f. to photoconductive resistance decrease is constant at strong illumination are shown to be in agreement with the theoretical treatment. Measurements of bulk photo e. m. f. as a function of temperature show a qualitative agreement with theory at low temperatures (extrinsic range). At high temperatures (intrinsic range) the results show a close agreement with the theoretically predicted behaviour.

GRADUATE STUDIES

Field of Study: Physics

Graduate Courses outside the Physics Department:

Network Theory,	A. D. Moore,	Electrical Engineering
Servomechanisms,	E. V. Bohn,	Electrical Engineering
Theory of Alloys	V. Griffiths,	Metallurgy

PUBLICATIONS

M.W. Johns, C.D. Cox, C.C. MacMullen, The Spins of Excited States of Cd^{114}, Physical Review 86, 632 (1952)

M.W. Johns, C.D. Cox, R.J. Donnelly, C.C. MacMullen, Radioactive Decay of In^{114}, Physical Review 87, 1134 (1952)

M.W. Johns, H. Waterman, D. MacAskill, C.D. Cox, A. Description of a Large Double-Focussing Beta Spectrometer and Its Application to a Study of the Decay of In^{114}, Canadian Journal of Physics, 31, 225 (1953).

BULK PHOTO-EFFECTS IN INHOMOGENEOUS SEMICONDUCTORS

by

CLARENCE DONALD COX

B.Sc., University of New Brunswick, 1950
M.Sc., McMaster University, 1952

A THESIS SUBMITTED IN PARTIAL FULFILMENT OF

THE REQUIREMENTS FOR THE DEGREE OF

DOCTOR OF PHILOSOPHY

in the Department

of

Physics

We accept this thesis as conforming to the

required standard

THE UNIVERSITY OF BRITISH COLUMBIA

May, 1959

A B S T R A C T

An observable e.m.f. exists in a semiconductor when a non-equilibrium carrier concentration is present in a region of electrostatic potential gradient. These two conditions may arise in a variety of ways, and the e.m.f.'s associated with various combinations of conditions are listed. One of these e.m.f.'s arises from a photo-generated non-equilibrium carrier concentration in regions of electrostatic potential gradient due to an inhomogeneous impurity distribution. The thesis is chiefly concerned with the extension of the theory of this bulk photo e.m.f. and its comparison with experiment.

Previous work on the subject is reviewed and the theory is developed to cover all conditions of illumination in the region of an arbitrary impurity density gradient. An expression for the bulk photo e.m.f. is derived by two approaches, integration of the electrostatic potential gradient, and integration of the carrier quasi Fermi levels, over the illuminated region. The latter derivation is shown to be more general in its application, and is used to obtain an expression for the photo e.m.f. both in an illuminated p-n junction and in an illuminated bulk inhomogeneity. Using the general result, expressions for the e.m.f. are written for the extreme cases of weak and strong illumination in extrinsic and nearly intrinsic semiconductors. The relation between bulk photo e.m.f. and photoconductive resistance decrease is examined.

Measurements were made of the bulk photo e.m.f. as a function of light intensity. The proportionality of the effect at low levels of illumination was verified. Observations of the photo e.m.f. patterns showed a maximum of e.m.f. at positions of maximum conductivity gradient. Since the bulk photo e.m.f. is a function of conductivity gradient, light probe measurements give a sensitive technique for the detection of inhomogeneous impurity distributions. With weak illumination, the measured ratio of photo e.m.f. to photoconductive resistance decrease was a constant independent of light intensity. These observations verified the theory and suggested a use for this ratio in quantitative measurements of conductivity gradient. The photo e.m.f. at strong illumination was shown to be dependent on the impurity distribution outside the region of incident light. The conditions under which the ratio of photo e.m.f. to photoconductive resistance decrease is constant at strong illumination are shown to be in agreement with the theoretical treatment. Measurements of bulk photo e.m.f. as a function of temperature show a qualitative agreement with theory at low temperatures (extrinsic range). At high temperatures (intrinsic range) the results show a close agreement with the theoretically predicted behaviour.

In presenting this thesis in partial fulfilment of the requirements for an advanced degree at the University of British Columbia, I agree that the Library shall make it freely available for reference and study. I further agree that permission for extensive copying of this thesis for scholarly purposes may be granted by the Head of my Department or by his representatives. It is understood that copying or publication of this thesis for financial gain shall not be allowed without my written permission.

Department of _____Physics_____

The University of British Columbia,
Vancouver 8, Canada.

Date _____June 12, 1959_____

TABLE OF CONTENTS

L I S T   O F   F I G U R E S

A C K N O W L E D G M E N T S

CHAPTER 1 - INTRODUCTION

1.1 Intrinsic and Extrinsic Semiconductors

An electron moving in a crystal is subject to a periodic potential arising from the atoms of the lattice. Quantum mechanics shows that an electron moving in such a periodic potential has certain ranges or bands of allowed energy states. If a band is incompletely filled the crystal will have a metallic character; on the other hand, if a certain number of bands are completely full the electrons are not available for conduction, and the material will be an insulator at absolute zero. At temperatures other than zero, some electrons in the filled band (valence band) will be excited into the next highest empty band (conduction band). If the forbidden energy gap is several electron volts wide, the material will remain an insulator for all practical purposes. For a forbidden gap of the order of one electron volt or less, however, a considerable number of thermally excited electrons appear in the conduction band at room temperature and the material is classified as a semiconductor. When an electron becomes available for conduction by excitation across the forbidden gap, a vacancy occurs in the valence band. This vacancy or hole can also contribute to conduction, and behaves like a particle with positive mass and charge.

An intrinsic semiconductor has an equal number of electrons and holes, i.e., the carriers have all been

produced by excitation of electrons from the valence to
the conduction band, and the electrical conductivity is
an intrinsic characteristic of the substance. However,
most semiconductors owe their conductivity to impurities,
and these may be classified electrically as donors or
acceptors. A donor impurity donates an electron to the
conduction band while an acceptor traps an electron from the
valence band, freeing a hole. In either case, an ionized
impurity is left behind. When impurities of both types are
present, the donors (N_D) give up electrons to the acceptors
(N_A) producing an effective impurity concentration ($N_D - N_A$).
If the density (n) of electrons or (p) of holes originating
from impurities is large compared with the intrinsic concen-
tration (n_i), one speaks of extrinsic or impurity semi-
conductors. The intrinsic concentration is a rapidly increas-
ing function of temperature and at a sufficiently high
temperature, all semiconductors will show intrinsic
characteristics. For the same reason, since no crystal can
be entirely free from impurities, sufficiently low tempera-
tures will produce some extrinsic behaviour.

Since electron and hole densities are partly
intrinsic and partly extrinsic in origin it is often convenient
to express them in terms of impurity density and intrinsic
concentration. Assuming electrical neutrality and complete
impurity ionization, we may equate positive and negative
charges in the crystal.

$$n + N_A = p + N_D$$

The generation and recombination of electrons and holes is a reversible pseudo-chemical reaction, and application of the mass action law gives

$$np = constant = n_i^2$$

These equations may be solved simultaneously to give carrier concentration in terms of impurity density and intrinsic concentration.

$$n = \left[\frac{N_D - N_A}{2}\right] + \sqrt{\left[\frac{N_D - N_A}{2}\right]^2 + n_i^2}$$

$$p = -\left[\frac{N_D - N_A}{2}\right] + \sqrt{\left[\frac{N_D - N_A}{2}\right]^2 + n_i^2}$$

Complete impurity ionization is a valid assumption in germanium except at very low temperatures, providing the impurities are predominantly the trivalent and pentavalent acceptor and donor elements which have very small activation energies (less than kT). At all points in the crystal, any separation of carrier types sets up a counteracting field tending to restore electrical balance, and electrical neutrality may be assumed except in regions of abrupt impurity density gradient (Shockley 1949), and even here significant departures from neutrality exist only in narrow regions.

1.2 Semiconductor Impurities

Impurities may be chemical or physical in origin, i.e., foreign elements or crystal imperfections. In the group IV semiconductors for example, the group III and V elements act as acceptors and donors respectively, and enter the lattice substitutionally (Pearson 1949). This is explained in terms of the valence electron structure of these elements (Shockley 1950). On the other hand, copper and nickel take up interstitial positions and behave as acceptors, and there is some evidence that copper substitutionally acts as a donor. The impurity characteristics of these elements are not thoroughly understood.

Crystal imperfections may be produced by plastic deformation or radiation, or may occur during the crystal growth. These imperfections can act as donor and acceptor centers. Experimental evidence suggests that lattice vacancies act as acceptors and interstitial atoms as donors. Dislocations produced by plastic deformation or other means act as acceptor centers. This characteristic is identified with the unpaired electrons on the edge of the extra atomic plane of a dislocation. These tend to trap free electrons and form "dangling bonds" (Read 1954). When these acceptor levels are ionized the dislocation acts like a line of negative charge and scattering of electrons by charged dislocations affects the mobility of carriers in the crystal (Read 1955). Lattice stress in the neighbourhood of a

dislocation causes local distortion of the band edges
(Chynoweth 1958).

1.3 Generation of e.m.f. in Semiconductors

Concentrations of electrons and holes in thermal equilibrium can be calculated by integrating the product of the Fermi function and density of states over the range of available energies. If the Fermi level is located in the energy gap several kT from a band edge, the Fermi function can be approximated by a Boltzmann factor, giving the familiar non-degenerate form of the carrier concentrations. Carrier densities may be alternatively expressed as the product of intrinsic concentration and a Boltzmann factor in which the energy term involves the difference of Fermi level and electrostatic potential in the exponent (Shockley 1950). Semiconductor parameters such as effective mass, energy gap, and density of energy states are implicit in the intrinsic concentration provided the bands have a simple parabolic energy versus momentum dependence.

If two regions of a semiconductor in thermal equilibrium have different carrier densities, there will be a gradient of electrostatic potential or "inner electric field" between these regions. According to the principle of detailed balance, the drift current associated with holes moving in this field is exactly balanced by an equal and opposite hole diffusion current, and the same current balancing applies to electron currents. Thus the gradient of electrostatic potential in the crystal will be the sum of any externally applied and inner electric fields. In the following pages, electrostatic potential is related to

conditions in the crystal, and e.m.f. or voltage to externally observed or applied potential differences. If a semiconductor in equilibrium has an electrostatic potential gradient, it can effect a charge separation of injected carriers which appears as an externally observable e.m.f. In general, e.m.f.'s will exist when a non-equilibrium carrier concentration is present in a region of electrostatic potential gradient.

Non-equilibrium carrier concentrations are produced by optical or thermal excitation, particle bombardment, or injection. Electrostatic potential gradients exist with impurity density gradients, energy gap variations, thermal gradient, or inhomogeneous magnetic fields through splitting of energy levels in the bands. Thus there are a considerable number of possibilities of e.m.f. generation with various combinations of these two sets of conditions. Many of them, however, are negligibly small, or cannot be observed separately. For example, thermal gradients produce an electrostatic potential gradient and also a gradient in energy gap. The relative contributions of these to an e.m.f. may be calculated but the effects cannot be separately observed. An e.m.f. from particle bombardment of a p-n junction has been observed, but for particle energies above a threshold value, a particle flux sufficient to produce measureable e.m.f.'s would seriously damage the crystal under observation.

Since an electrostatic potential gradient is always

associated with some spatial gradient of physical charac-
teristics of the semiconductor, an e.m.f. arising from
thermal gradient may be classified as a thermocouple effect.
Conditions which give rise to electrostatic potential
gradients also produce a change of carrier mobilities, and
Tauc (1957) has shown that a change of mobility ratio over
the region of non-equilibrium carrier concentration will
also cause an e.m.f.   This effect, however, is negligible
compared with the e.m.f. from the electrostatic potential
gradient.

Most of the photo e.m.f.'s have been observed
and identified (Tauc 1957). Of these we will be chiefly
concerned with the photo e.m.f. due to illumination of a
region of impurity gradient.   The bulk photo e.m.f. and the
illuminated p-n junction may be considered as two extremes
of this effect.   In the case of the bulk photo e.m.f. the
electrostatic potential gradient is gradual, and electrical
neutrality may be assumed throughout the crystal, while in
the p-n junction there is a space charge region associated
with the abrupt impurity gradient, and the analyses of the
photo e.m.f. in the two cases are quite different, even
though they are fundamentally of the same origin.

CHAPTER 2 - THEORY OF BULK PHOTO E.M.F.'S

2.1 General

The equilibrium carrier concentrations in a non-degenerate semiconductor may be calculated by integrating the product of the density of energy states and the Boltzmann distribution over the range of available energies. Alternatively, we may define an electrostatic potential ψ_0 which is related to the energy of an electron (or hole) at rest in the conduction (or valence) band. For reasons of symmetry we make ψ_0 the energy of a unit charge placed at the level at which the Fermi energy would occur in the intrinsic semiconductor in thermal equilibrium. Then the equilibrium carrier concentrations have the form

$$n_o(x) = n_i \exp \frac{q}{kT} \left[\psi_o(x) - \phi_o \right]$$

$$p_o(x) = n_i \exp \frac{q}{kT} \left[\phi_o - \psi_o(x) \right]$$

Subscript zero refers to equilibrium conditions. Non-equilibrium densities are expressed by replacing the common Fermi level ϕ_0 by quasi-Fermi levels or imrefs ϕ_n and ϕ_p. Since the non-equilibrium value of the electrostatic potential is dependent on the carrier distribution, it is customary to consider it equal to the equilibrium value at some unperturbed point, and to specify all other values in terms of this point. The positional dependence of the

non-equilibrium electrostatic potential is not in general
equal to that in the equilibrium case, and this is indicated
by dropping the subscript zero.

In equilibrium the imrefs may be thought of as
coinciding with the Fermi level which is uniform throughout
the system. When the carrier concentrations are perturbed,
for instance by illumination, the imrefs separate, and take
up positions describing the new carrier densities. At
unperturbed points outside the illuminated region, the imrefs
return to the equilibrium Fermi level. If the region of non-
equilibrium gives rise to a difference of Fermi level between
two points a and b on either side of the disturbed region,
this difference is equal to the integral of either imref
gradient between the two points,

$$\phi(b) - \phi(a) = \int_a^b \text{grad} \ \phi_{n,p} \, dx$$

and may be identified with the voltage difference (or e.m.f.)
observed between the points a and b (Shockley 1950).

Electron and hole current densities may also be
expressed in terms of the imref gradients. Current densities
consist of a field induced or drift component and a diffusion
component involving the carrier density gradients. By
substituting for the carrier density gradients using the
above relationships, total current densities may be written

$$J_p = -q \, \mu_p \, p \, \text{grad} \ \phi_p$$

$$J_n = -q \, \mu_n \, n \, \text{grad} \ \phi_n$$

where μ_n and μ_p refer to electron and hole mobilities,

and the Einstein relation $\quad \dfrac{D_p}{\mu_p} = \dfrac{D_n}{\mu_n} = \dfrac{kT}{q}$

has been assumed valid. D_n and D_p are the electron and

hole diffusivities.

2.2 Imref Representations of Non-equilibrium Conditions

A non-equilibrium condition in a semiconductor can be graphically represented by an imref and electrostatic potential diagram. This will specify carrier concentrations, current densities, existing e.m.f.'s, and in fact contains a complete physical description of the electrical properties of the material. In undertaking an analysis of a semiconductor problem, a qualitative imref diagram can be helpful as was first demonstrated by Shockley (1950) for the p-n junction. Such a diagram, without being quantitatively exact until the solution is reached, can be consistent and provide information that is not always obvious. For instance, a qualitative imref representation can predict the polarity but not the value of an e.m.f. and the direction but not the magnitude of a current density. By appealing to fundamental principles, a set of conditions can be formulated to be used as a guide to consistent imref diagrams. These involve (i) the continuity equation, (ii) ratio of drift to diffusion current densities, and (iii) electrical neutrality.

(i) The continuity equations for electrons and holes are

$$\frac{\partial n}{\partial t} = (g - r) + \frac{1}{q} \operatorname{div} \vec{J_n}$$

$$\frac{\partial p}{\partial t} = (g - r) - \frac{1}{q} \operatorname{div} \vec{J_p}$$

where g and r are the rates per unit volume of generation
and recombination of carrier pairs. If the time derivatives
are zero and using one dimensional geometry these become

$$\frac{dJ_n}{dx} = -q(g-r)$$

$$\frac{dJ_p}{dx} = q(g-r)$$

One dimensional geometry will be a valid assumption in the
case of photo carrier excitation if the specimen is thin
enough that the carriers are generated uniformly throughout
the bulk under the illuminated area. We may also make this
assumption in a current carrying filament with low surface
recombination. Regions where generation and recombination
rates are different are easily identified, and the continuity
equations enable us to relate these regions to positional
change of the current densities and hence of the imrefs.

Where the time derivatives are equal we may write

$$J_n + J_p = J = constant$$

This helps in estimating the relative gradients of the imrefs.
In particular, if the total current is everywhere zero,

$$n\mu_n \, grad \, \phi_n = -p\mu_p \, grad \, \phi_p$$

and $$\frac{grad \, \phi_p}{grad \, \phi_n} = -\frac{bn}{p}$$

where b is the ratio of electron to hole mobilities.

With one-dimensional geometry the gradients depend on a single coordinate only, and may be considered vectors lying in the x-axis. Thus the products or quotients of gradients are scalar quantities with positive values when the gradients are in the same direction and negative values when they are in opposite directions.

(ii) The equations for total current densities consist of a drift and a diffusion term. The ratios of these terms are

$$\frac{\text{diff. } J_p}{\text{drift } J_p} = \frac{\text{grad}\,(\phi_p - \psi)}{\text{grad}\,\psi}$$

and

$$\frac{\text{diff. } J_n}{\text{drift } J_n} = \frac{\text{grad}\,(\phi_n - \psi)}{\text{grad}\,\psi}$$

If the current density is predominantly diffusional, the electrostatic potential gradient is approximately zero. When the drift current density predominates the gradients of imrefs and electrostatic potential are equal.

(iii) We assume crystal neutrality everywhere except in a junction transition layer, and therefore the imrefs must be consistent with an equal disturbance of the densities of both signs of carriers. The product of non-equilibrium carrier concentrations establishes the relative magnitude of the electron and hole imrefs.

$$np = n_i^2 \exp \frac{q}{kT} (\phi_p - \phi_n)$$

and hence
$$\phi_p - \phi_n = \frac{kT}{q} \ln\left(1 + \frac{\Delta n}{n_o}\right)\left(1 + \frac{\Delta p}{p_o}\right)$$

where Δn and Δp are the added densities of electrons and holes. Shockley (1949) has used an approximate form of this equation to obtain an expression for the injected minority carrier density in a biassed p-n junction. He assumes the added carrier density negligible compared with the majority carrier density, and thus in n-type material

$$p \doteq p_o \exp\frac{q}{kT}(\phi_p - \phi_n)$$

Misawa (1955) gives the exact form for the injected minority carrier densities. Using the neutrality condition, for instance in n material

$$n = n_o + p - p_o$$

so that

$$p\left(p + n_o - p_o\right) = n_i^2 \exp\frac{q}{kT}\left(\phi_p - \phi_n\right)$$

or

$$p\left[1 + \frac{p - p_o}{n_o}\right] = p_o \exp\frac{q}{kT}\left(\phi_p - \phi_n\right)$$

and the minority carrier density p is the solution of the above quadratic equation. Fletcher (1957) expresses non-equilibrium carrier densities in terms of the junction electrostatic potential step. However, his identification of the applied bias voltage as the difference of the

equilibrium and non-equilibrium potential step is incorrect.

A subsidiary condition is applicable when the generated or injected carrier densities are large compared with the equilibrium densities. In this case the imref gradients are inversely proportional to the ambipolar diffusion length. In extrinsic semiconductors where the added minority carrier densities are smaller than the equilibrium majority carrier density but large compared with the equilibrium minority density

$$\left| \text{grad } \phi_n \right| = \frac{kT}{qL_n}$$

$$\left| \text{grad } \phi_p \right| = \frac{kT}{qL_p}$$

where L_n and L_p are the electron and hole diffusion lengths (Appendix I).

HOMOGENEOUS n-TYPE SEMICONDUCTOR
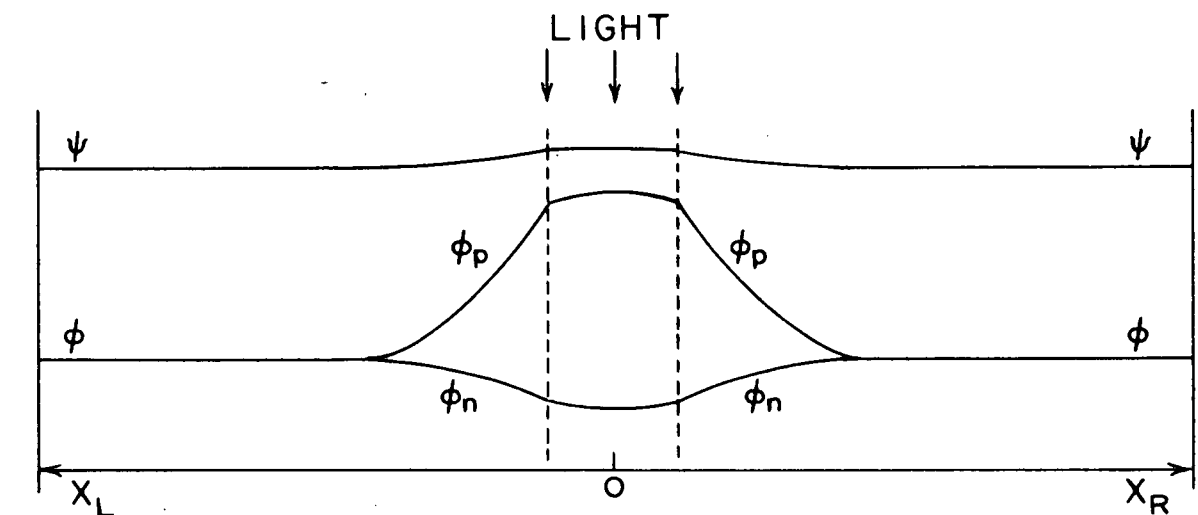
LIGHT

ψ ψ

ϕ_p ϕ_p

ϕ ϕ

ϕ_n ϕ_n

X_L O X_R

IMREFS AND ELECTROSTATIC POTENTIAL

J_L J_L

$g > r$

J_p J_n

O $r > g$ $r > g$

J_n J_p

J_R $g > r$ J_R

CURRENT DENSITIES

$\ln \frac{n, p}{n_i}$ $\ln \frac{n, p}{n_i}$

n n

O

p p

CARRIER CONCENTRATIONS

The imref diagrams (Figures 1 to 5) show how incident light modifies the imrefs and electrostatic potential, and can in some cases give rise to an e.m.f. These diagrams are qualitative and are primarily for purposes of illustration. For this reason the junction transition regions have been greatly expanded to show the behaviour of the imrefs and electrostatic potential in these regions, and except for the π-i-ν junction (Figure 4) the relative carrier densities are unspecified. The notations π and ν represent very small impurity densities of the p and n type respectively. Thus π and ν materials are nearly intrinsic and the π-i-ν junction is a "weak" p-n junction.

When a homogeneous semiconductor is illuminated (Figures 1 and 2) the imrefs separate and the electrostatic potential changes from its equilibrium value. The latter is caused by a difference in carrier mobilities. Electrons and holes generated in the illuminated volume diffuse away from the region of high concentration, and the electrons, having the greater mobility, will tend to move ahead of the holes. Such a tendency sets up an electric field which slows the electrons and speeds up the holes in their motion away from the illuminated region.

HOMOGENEOUS INTRINSIC SEMICONDUCTOR!
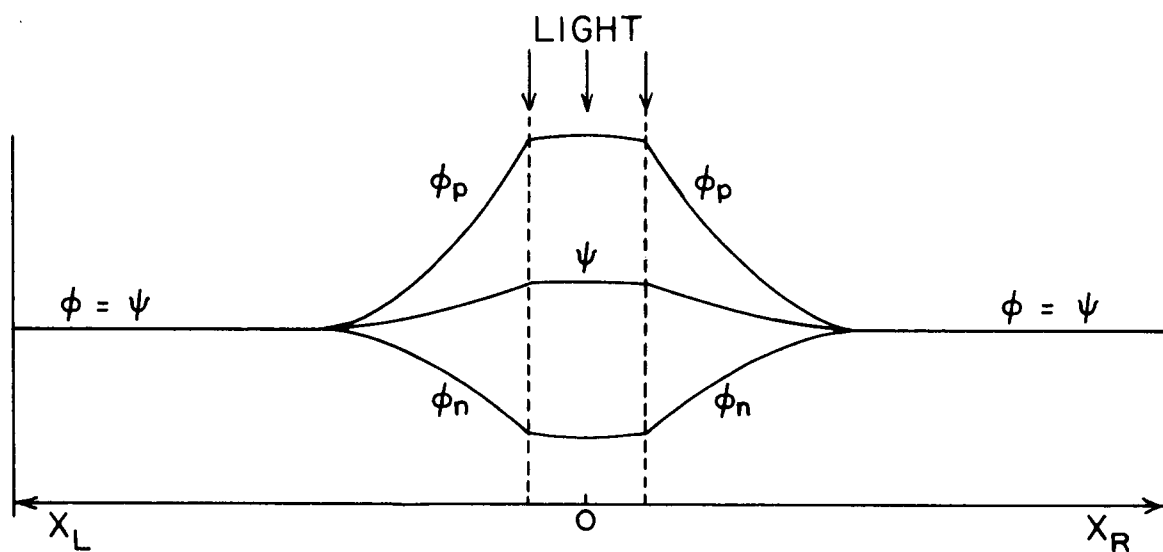
IMREFS AND ELECTROSTATIC POTENTIAL
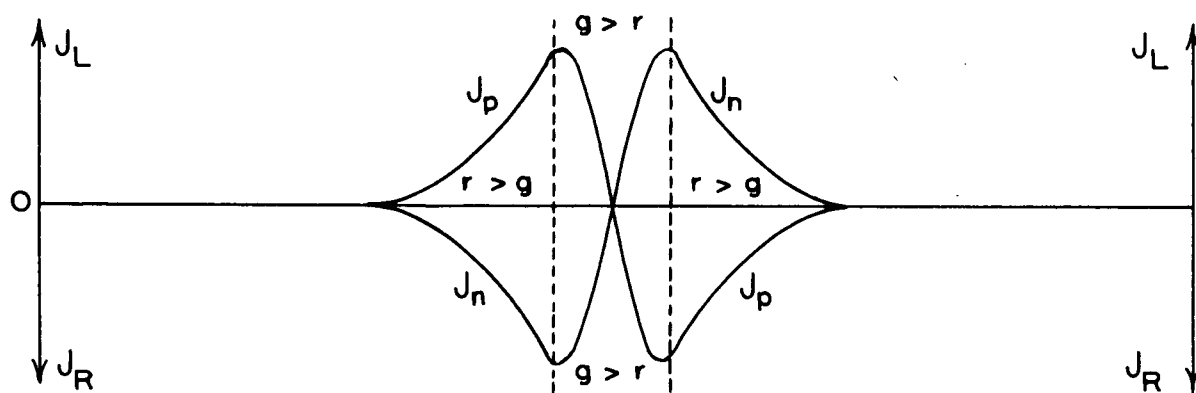
CURRENT DENSITIES
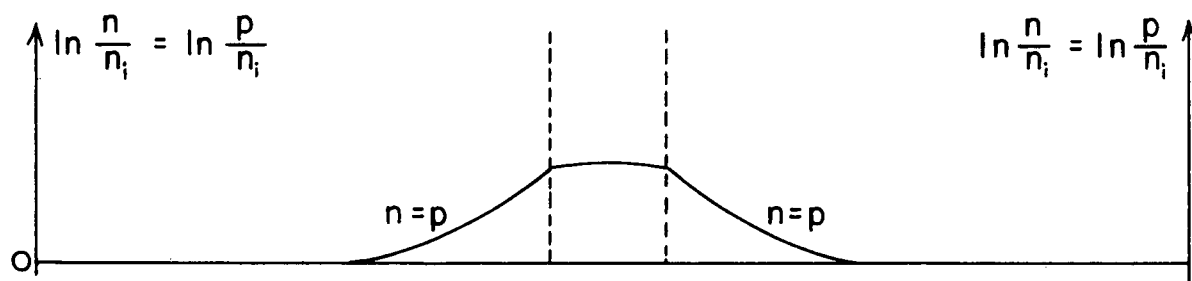
CARRIER CONCENTRATIONS

This field is identified with a gradient of the electrostatic potential under illumination (see Appendix II), and in a homogeneous semiconductor open circuited $(J=0)$

$$\text{grad } \psi = -\frac{(b-1)\text{ grad } \phi_n}{1 + \frac{p}{n}} = \frac{(b-1)\text{ grad } \phi_P}{b\left(1 + \frac{p}{n}\right)}$$

$$= (b-1)\frac{kT}{q}\frac{\text{grad } \Delta n}{bn+p}$$

Thus for a given illumination, the gradient of electrostatic potential will be most pronounced in an intrinsic semiconductor (Figure 2) where

$$\text{grad } \psi = \frac{(b-1)}{(b+1)}\frac{kT}{q}\frac{\text{grad } \Delta n}{n}$$

In n-type (Figure 1)

$$\text{grad } \psi \doteq -(b-1)\text{ grad } \phi_n$$

In the illuminated region where generation exceeds recombination, the space derivative of hole current density is positive and that of electron current density negative in accordance with condition (i). The opposite holds where recombination is greater than generation. In homogeneous illuminated semiconductors the current densities are symmetrical about the mid-point of illumination, provided that surface conditions are uniform and light intensity is constant over the illuminated regions.

FIGURE 3

p-n JUNCTION (OPEN CIRCUIT)

IMREFS AND ELECTROSTATIC POTENTIAL

CURRENT DENSITIES

CARRIER CONCENTRATIONS

In the illuminated p-n junction (Figure 3) carriers
generated in the transition region separate because of the
inner electric field and a photo e.m.f. is observed. The
added majority carrier density is usually small compared
with the equilibrium density and diffusional effects cause
a negligible perturbation of the electrostatic potential.
This is illustrated in Figure 3, in the carrier concentra-
tion and imref diagrams. Total current densities are zero
everywhere, but the current densities are not necessarily
symmetrical about the x = 0 plane, since diffusion lengths
are normally not equal in the p and n materials.

FIGURE 4

$\pi-i-\nu$ JUNCTION (OPEN CIRCUIT)
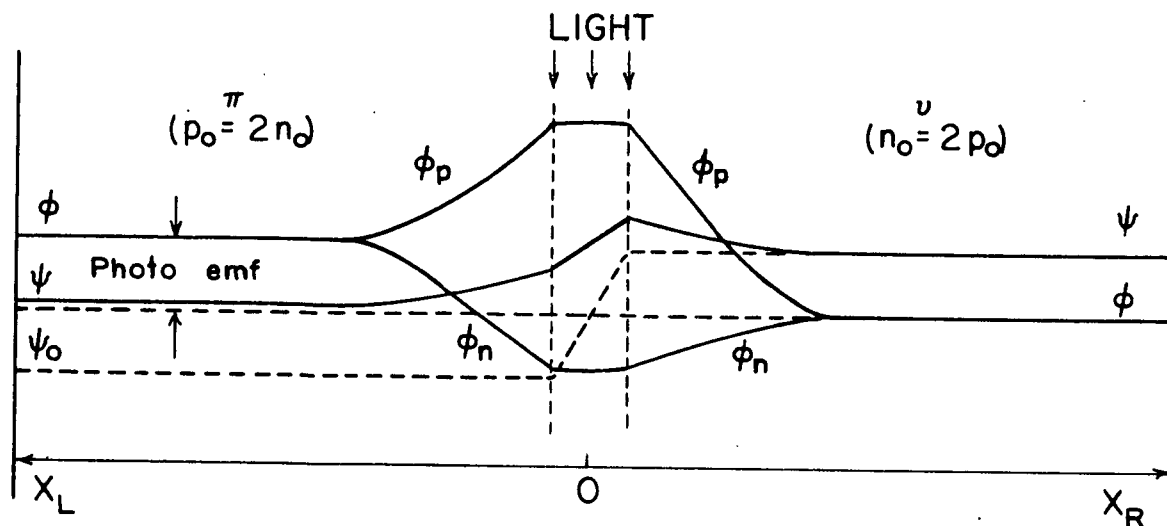
IMREFS AND ELECTROSTATIC POTENTIAL
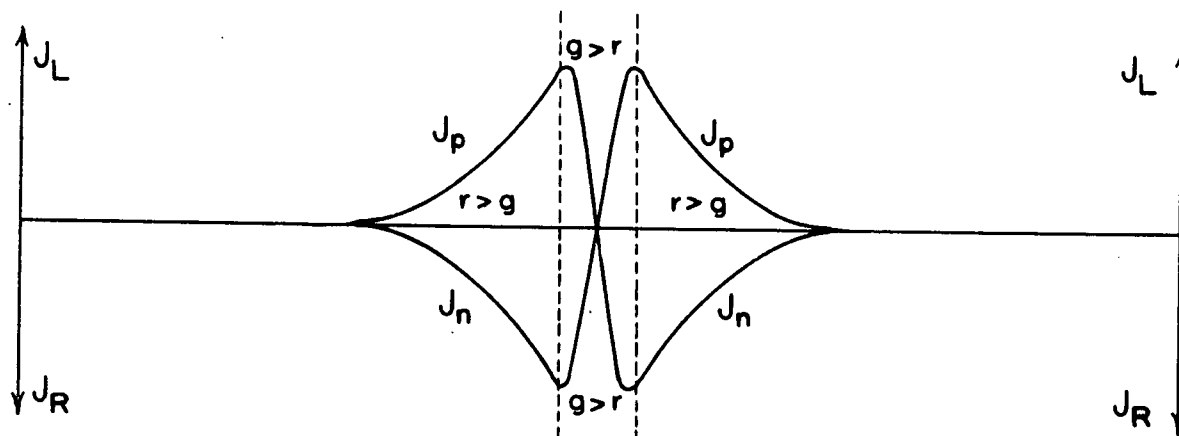
CURRENT DENSITIES
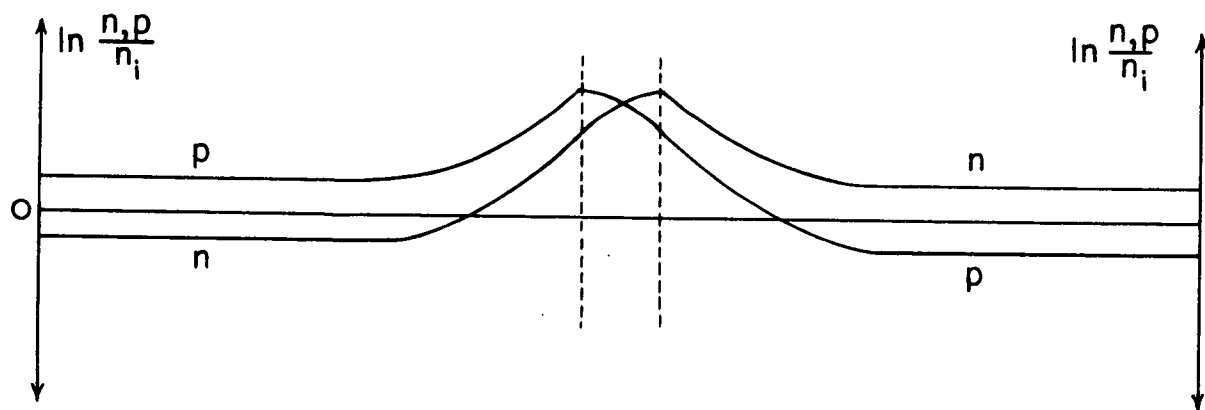
CARRIER CONCENTRATIONS

The weak p-n (or $\pi - i - \nu$) junction (Figure 4) shows a considerable perturbation of the electrostatic potential under illumination, and these perturbations are not equal on the two sides of the junction. Thus the resulting photo e.m.f. is partly diffusional in origin. The differences of imrefs and electrostatic potential at the edge of the transition layer have been drawn to correspond to equilibrium hole density in the π side equal to twice the electron density, and an equilibrium electron density in the ν side equal to twice that of the holes. Although the π and ν materials are very nearly intrinsic there is a marked asymmetry of imrefs on either side of the junction. The diffusion lengths will be approximately equal, and consequently the current densities are symmetrical about x = 0.

FIGURE 5

BULK INHOMOGENEITY (OPEN CIRCUIT)

IMREFS AND ELECTROSTATIC POTENTIAL

CURRENT DENSITIES

CARRIER CONCENTRATIONS
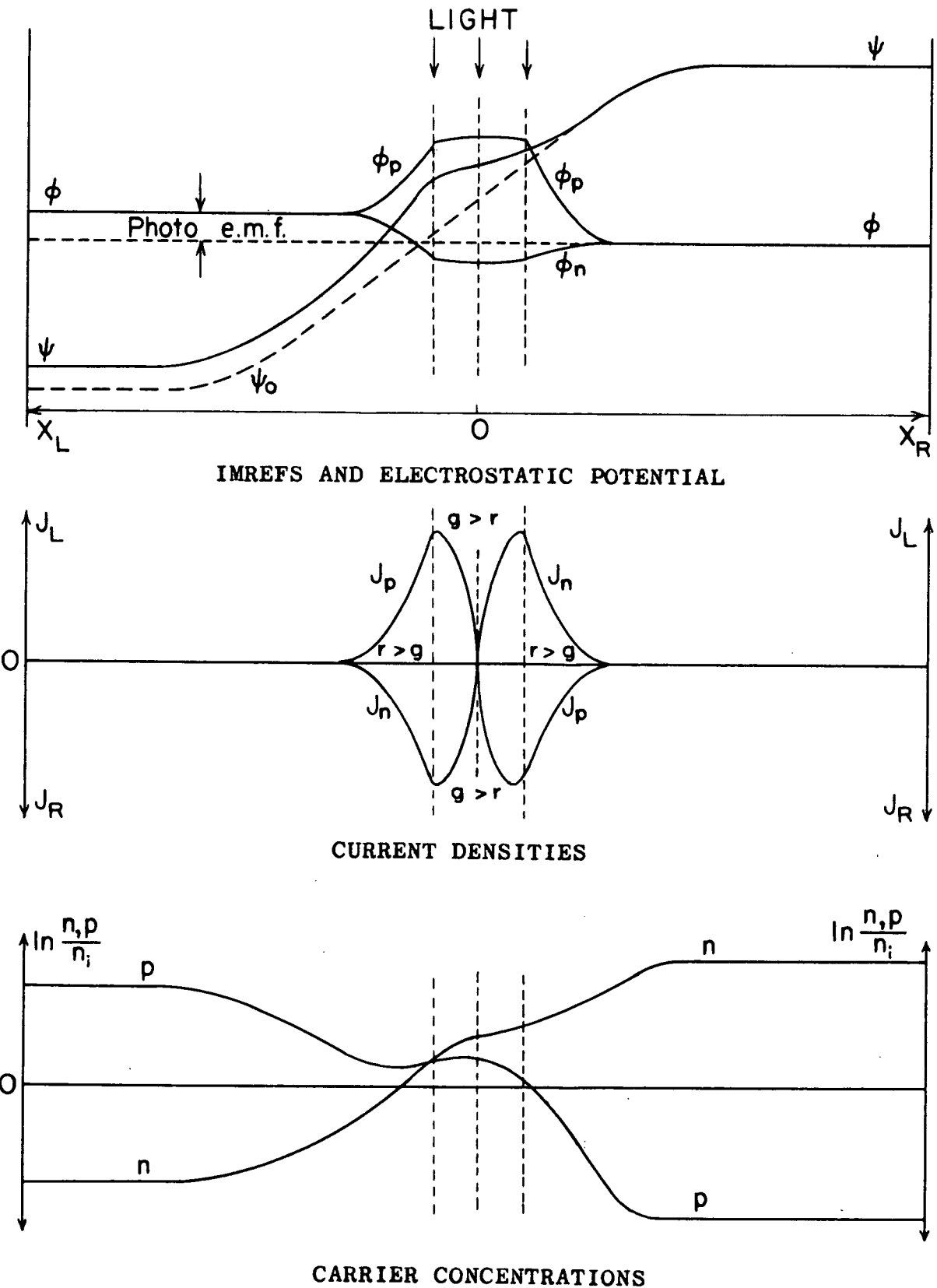
The bulk photo e.m.f. arises from illumination of a gradual impurity density gradient (Figure 5). The diagram is drawn for n material and the chief component of e.m.f. arises from the difference of electrostatic potential at the illumination edges. As light intensity increases, the electrostatic potential gradient in the illuminated region approaches zero. However, the diffusional perturbations of e.m.f. on either side of the illuminated region are unequal, and the maximum e.m.f. will always be less than the difference between the values of equilibrium electrostatic potential at the illumination edges. Since we assume the impurity gradient is gradual, the diffusion lengths on either side of the illuminated region are approximately equal and the current densities are symmetrical about $x = 0$.

2.3 Analysis of the Bulk e.m.f.

A theoretical analysis of the e.m.f. arising from illumination of an impurity gradient in a semiconductor was first published by Tauc (1955). Briefly, his derivation of an expression for the bulk photo e.m.f. involves integrating the gradient of electrostatic potential between two unperturbed points on either side of the illuminated region. This yields an expression for the bulk photo e.m.f. provided that the equilibrium electrostatic potential is the same at the integration limits.

$$e_B = \int_a^b grad \ \psi \ dx$$

if

$$\psi_o(b) = \psi_o(a)$$

We have followed Tauc in making six basic assumptions and these are included below for critical examination.

(a) Electrical neutrality is assumed for both illuminated and equilibrium conditions, except in regions of abrupt impurity density gradients such as occur in p-n junctions. It should be emphasized that this assumption represents only a close approximation to electrical conditions in the crystal since a tendency towards charge separation is the agency which sets up opposing inner fields, i.e., electrostatic potential gradients. However, except in semiconductor junctions, space charge effects are

negligible and the crystal may be assumed electrically neutral. (Gunn 1958). The postulate of neutrality implies ambipolar carrier mobility (Rittner 1954) which is automatically taken into account in the analysis of the bulk photo e.m.f. and gives rise to factors involving the mobility ratio.

(b) Impurity atoms are assumed totally ionized. This assumption simplifies the mathematical treatment but its validity depends both on the semiconductor and the impurity. In germanium the activation energies of most impurities are small enough that ionization is essentially complete, and this assumption is valid in our work.

(c) Classical statistics are assumed in both the dark and illuminated regions. The most intense illumination used in the experimental studies was not sufficient to approach degeneracy since the added carrier density was estimated never to have exceeded $10^{16} cm^{-3}$.

(d) Ratio of electron to hole mobility is assumed constant. This assumption holds for all illuminations used since hole-electron scattering would not be significant.

(e) Uniform generation of photo carriers is assumed across the bulk of the semiconductor. Using this assumption, the theoretical analysis becomes one-dimensional and gradients depend on a single coordinate only. This is not the case experimentally, but from the data it would appear that this assumption is not particularly restrictive.

(f) Added carrier concentration is assumed zero

FIGURE 6

ASSUMED CARRIER DISTRIBUTION IN AN

ILLUMINATED BULK INHOMOGENEITY
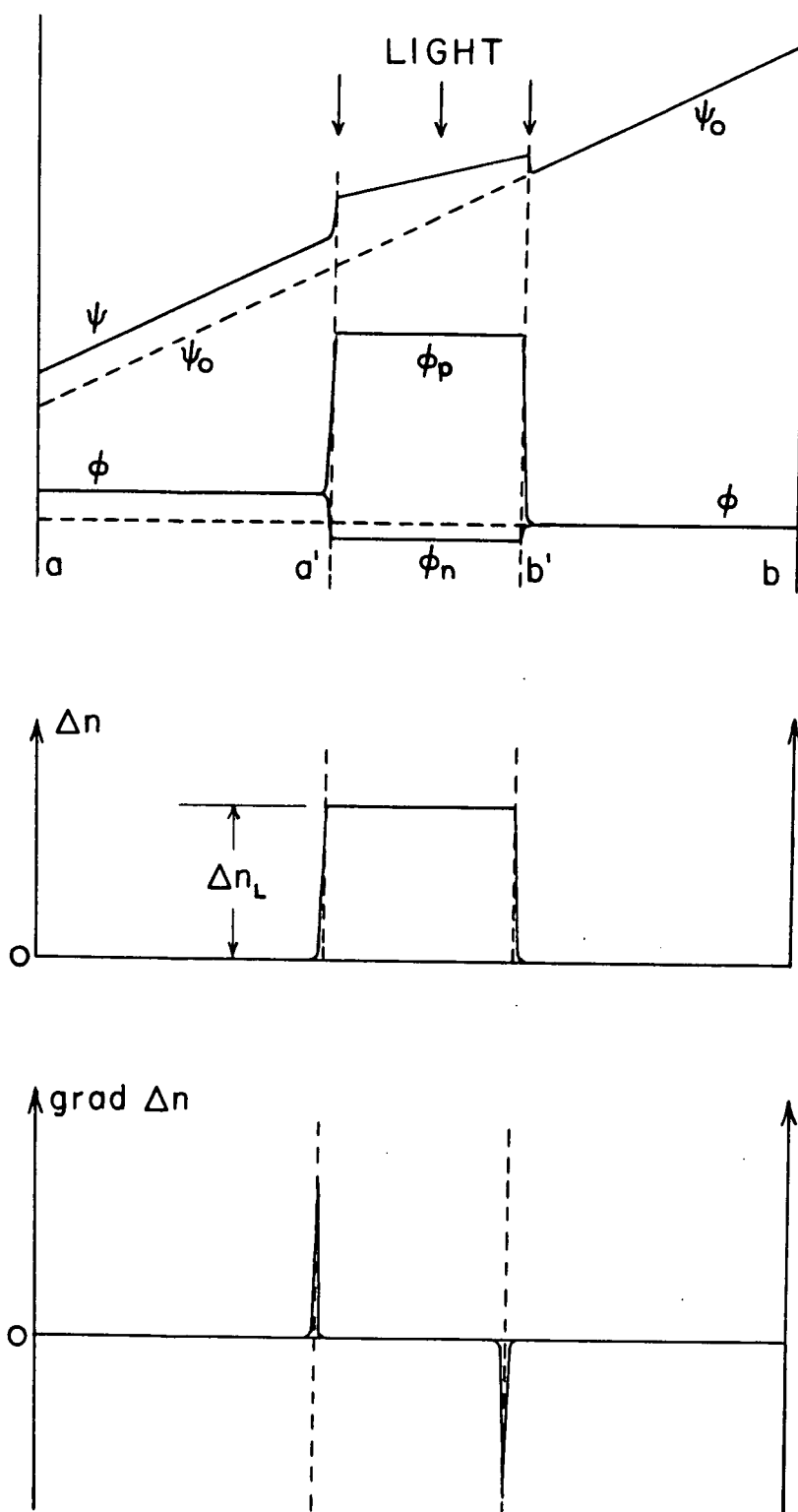
outside a region which is ordinarily identified with
the illuminated region, and is assumed constant within the
illuminated region. This assumption simplifies the analysis
of the bulk photo e.m.f., and its implications are
discussed in detail at the end of this section.

(g) An additional assumption is implicit in Tauc's
work but is not stated, i.e., carrier lifetime is assumed
constant. This holds for weak illuminations, but for large
added carrier density lifetime becomes a function of carrier
concentration. This implies that the excess carrier density
due to illumination will not be a linear function of the
illumination.

The e.m.f. which exists through illumination of
a region of impurity density gradient may be expressed either
in terms of the disturbance of the carrier imrefs or
electrostatic potential. This is illustrated in Figure 6
for the case of a bulk inhomogeneity. When a region of
inhomogeneity is illuminated between the points a' and b',
the bulk photo voltage e_B between unperturbed points a and
b is

$$e_B = \int_a^b grad\, \phi_p\, dx = \int_a^b grad\, \phi_n\, dx = \int_a^b grad(\psi - \psi_0)\, dx$$

These integrals are entirely general, and apply wherever an
e.m.f. arises from a non-equilibrium carrier density in a
region of electrostatic potential gradient. However for

physical reasons their evaluation is not always possible. In the p-n junction for instance, electrical neutrality does not hold in the transition region where the electric field is non-uniform, and thus the integral involving this quantity cannot be simply evaluated. In the following we will derive an expression for the bulk photo e.m.f. using the integrals of the electrostatic potential gradient, and also using the integral of the imref gradient. The former is essentially Tauc's (1957) method, although the approach is somewhat different, and this will be evaluated first.

By differentiating the expressions for non-equilibrium carrier concentrations, the imref gradients may be written

$$\text{grad } \phi_p = \text{grad } \psi + \frac{kT}{q} \frac{\text{grad } p}{p}$$

$$\text{grad } \phi_n = \text{grad } \psi - \frac{kT}{q} \frac{\text{grad } n}{n}$$

In the open circuit condition, total current is zero and

$$\frac{\text{grad } \phi_p}{\text{grad } \phi_n} = -\frac{bn}{p}$$

Dividing the above two equations and substituting for the ratio of imref gradients

$$\text{grad } \psi = \frac{kT}{q} \frac{b \text{ grad } n - \text{grad } p}{bn + p}$$

In equilibrium

$$grad\ \psi_0 = \frac{kT}{q}\ \frac{grad\ n_0}{n_0}$$

and from these, assuming $grad\Delta n = grad\Delta p$

$$\int_a^b grad\ (\psi - \psi_0)\ dx$$

$$= \frac{kT}{q} \int_a^b \left[\frac{(b-1)\ grad\ \Delta n}{p_0 + bn_0 + (b+1)\Delta n} - \frac{(b+1)\Delta n\ grad\ n_0}{bn_0^2 + \Delta n(b+1)n_0 + n_i^2} \right] dx$$

The integrands exist only where an added carrier concentration combined with an internal field exists or where a gradient of added carrier concentration exists, and this must be taken into consideration when the integrals are evaluated. The integration limits are arbitrarily chosen as two unperturbed points a and b on either side of the illuminated region. The equilibrium carrier densities at these points are not, however, involved in the solution since Δn and grad Δn are zero there. Thus the equilibrium carrier densities which appear in the solution will be the densities at the edges of illumination. The term involving the gradient of added carrier concentration is identified with e_d, the diffusional component of the e.m.f., and the term involving the gradients of the equilibrium carrier densities with e_c, the internal field component. The

integrals when evaluated (see Appendix III) give

$$e_d = \frac{kT}{q} \frac{(b-1)}{(b+1)} \ln \frac{1 + (b+1)\Delta n_L / p_{oa'} + b n_{oa'}}{1 + (b+1)\Delta n_L / p_{ob'} + b n_{ob'}}$$

and

$$e_c = -\frac{2kT}{q} \frac{(b+1)\Delta n_L}{\sqrt{D}} \left[\text{Tan}^{-1} \frac{2 b n_o + \Delta n_L (b+1)}{\sqrt{D}} \right]_{a'}^{b'}$$

when D is positive

$$e_c = -\frac{kT}{q} \frac{(b+1)\Delta n_L}{\sqrt{-D}} \left[\ln \frac{2 b n_o + (b+1)\Delta n_L - \sqrt{-D}}{2 b n_o + (b+1)\Delta n_L + \sqrt{-D}} \right]_{a'}^{b'}$$

when D is negative

where $D = 4 n_i^2 b - (b+1)^2 \Delta n_L^2$

where Δn_L , a constant, is the added carrier concentration within the illuminated region. The above expressions are simplified (see Appendix III) in the case of

(i) weak illumination $\left(\Delta n_L \ll p_0 + b n_0\right)$

$$e_B = e_d + e_c = \frac{2kT}{qb} \Delta n_L \left[\frac{1}{n_{ob'}} - \frac{1}{n_{oa'}}\right]$$

in n-type $\left(b n_0 \gg p_0\right)$

$$e_B = e_d + e_c = -\frac{2bkT}{q} \Delta n_L \left[\frac{1}{p_{ob'}} - \frac{1}{p_{oa'}}\right]$$

in p-type $\left(p_0 \gg b n_0\right)$

(ii) strong illumination $\left(\Delta n_L \gg p_0 + b n_0\right)$

$$e_B = e_d + e_c = -\frac{kT}{q} \frac{2}{b+1} \ln \frac{n_{ob'}}{n_{oa'}} \qquad \text{in n-type}$$

$$e_B = e_d + e_c = \frac{kT}{q} \frac{2b}{b+1} \ln \frac{p_{ob'}}{p_{oa'}} \qquad \text{in p-type}$$

These expressions can also be derived by applying
the appropriate approximations before the integral is
evaluated, and the integration is much simpler in this
case. The complete integral however, involves no assump-
tions as to the ratio n_0/p_0 and provides a convenient check
on the derivation of the e.m.f. through the imrefs.

Derivation of an expression for the bulk photo
e.m.f. using the imrefs involves the same general approach
used above.

$$e_B = \int_a^b \text{grad } \phi_n \, dx = \int_a^b \text{grad } \phi_p \, dx$$

and the imref gradients are expressed in terms of carrier densities and their gradients (see Appendix IV)

$$\text{grad } \phi_n = -\frac{kT}{q} \frac{1}{n} \frac{\text{grad}(np)}{bn+p}$$

$$\text{grad } \phi_p = \frac{bkT}{q} \frac{1}{p} \frac{\text{grad}(np)}{bn+p}$$

under open circuit conditions. These are expanded and expressed as the sum of terms involving gradient of added carrier density and gradient of equilibrium carrier densities. The integration between limits a and b gives (see Appendix IV)

$$e_d = -\frac{kT}{q} \ln\left[\frac{n_{oa'} + \Delta n_L}{n_{oa'}} \frac{n_{ob'}}{n_{ob'} + \Delta n_L} \right]$$

$$+ \frac{kT}{q} \frac{b-1}{b+1} \ln \frac{1 + (b+1)\Delta n_L \big/ p_{oa'} + b n_{oa'}}{1 + (b+1)\Delta n_L \big/ p_{ob'} + b n_{ob'}}$$

$$e_c = \frac{kT}{q} \ln\left[\frac{n_{ob'}}{n_{oa'}} \frac{n_{oa'} + \Delta n_L}{n_{ob'} + \Delta n_L} \right]$$

$$- \frac{2kT}{q} \frac{\Delta n_L (b+1)}{\sqrt{D}} \left[\text{Tan}^{-1} \frac{2 b n_o + \Delta n_L (b+1)}{\sqrt{D}} \right]_{a'}^{b'}$$

where $D = 4n_i^2 b - (b+1)^2 \Delta n_L^2$

In the case of the bulk photo e.m.f., the first terms of the diffusional and inner field components of e.m.f. cancel giving an expression for the bulk photo e.m.f. identical with that derived from the integral of the electrostatic potential gradients. The same final solution is also obtained from an integration of the hole imref over the illuminated region.

In the gradual bulk inhomogeneity the electrostatic potential is a slowly varying function of position and the approximations $\delta n_o \gg p_o$ in n-type material and $p_o \gg \delta n_o$ in p-type material may be introduced in the integrand when the photo e.m.f. is derived using the electrostatic potential gradient. The imref gradient however, is a rapidly varying non-monotonic function with opposite and almost equal excursions near the edges of illumination and the above approximations are not valid when applied to the integrand.

In both derivations the analysis is simplified by assumption (f), added carrier density is zero outside the illuminated region and constant within it (Figure 6). This implies the following approximation: gradient of added carrier density is small compared with gradient of equilibrium carrier density in the illuminated region, and at the edges the equilibrium carrier densities do not

change over the region of significant added carrier density gradient. Using this approximation, the e.m.f. integral is separated into two terms involving different variables, n_0 inside the illuminated region and Δn at the edges, and these terms are identified with the inner field and diffusional components of e.m.f. respectively.

However, when the width of the illuminated region is of the order of a diffusion length, the actual added carrier density distribution will be quite different from the assumed rectangular one, and n_0 may change appreciably over the region of significant grad Δn. The validity of assumption (f) and the form of the e.m.f. integrals will be examined under these conditions.

When a semiconductor is uniformly illuminated between points -a and a, the added carrier densities are (see Appendix V)

$$\Delta n = \frac{G \tau_p}{2} \left[1 - \exp \frac{-2a}{L_p} \right] \exp \frac{a - x}{L_p} \qquad (x > a)$$

$$\Delta n = \frac{G \tau_p}{2} \left[1 - \exp \frac{-2a}{L_p} \right] \exp \frac{a + x}{L_p} \qquad (x < -a)$$

$$\Delta n = G \tau_p \left[1 - \exp \frac{-a}{L_p} \cosh \frac{x}{L_p} \right] \qquad (-a < x < a)$$

where G is the rate of photo generation of carrier pairs per unit volume between points a and -a, τ_p and L_p are hole lifetimes and diffusion lengths.

CARRIER DISTRIBUTIONS IN AN ILLUMINATED
HOMOGENEOUS SEMICONDUCTOR

$a = 10 L_p \begin{cases} G \tau_p \times 100 \\ \Delta n \times 100 \end{cases}$

$\left. \begin{matrix} G \tau_p \\ \Delta n \end{matrix} \right\} \, a = L_p$

$-X$ $-a$ O a X

CARRIER CONCENTRATIONS

$a = 10 L_p$

$a = L_p$

$-X$ $-a$ O a X
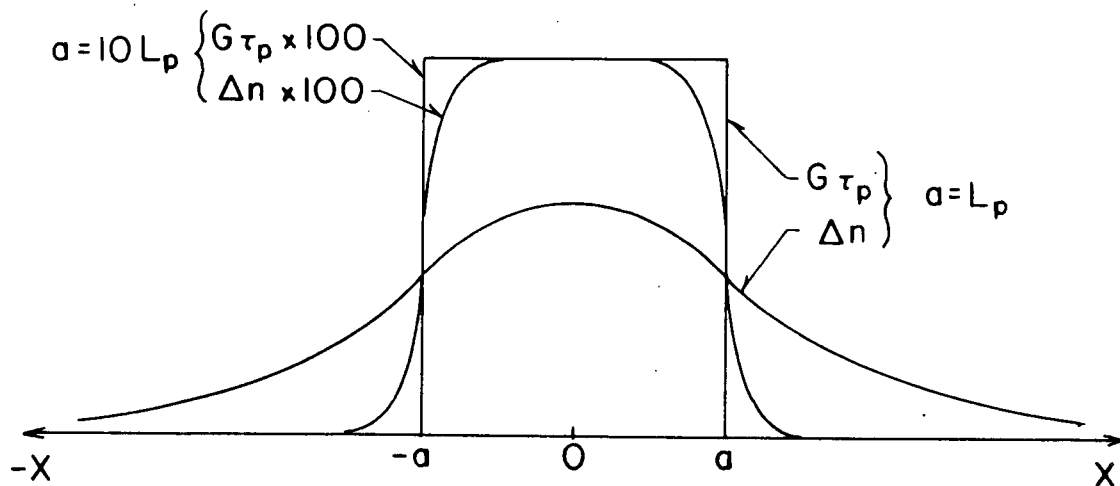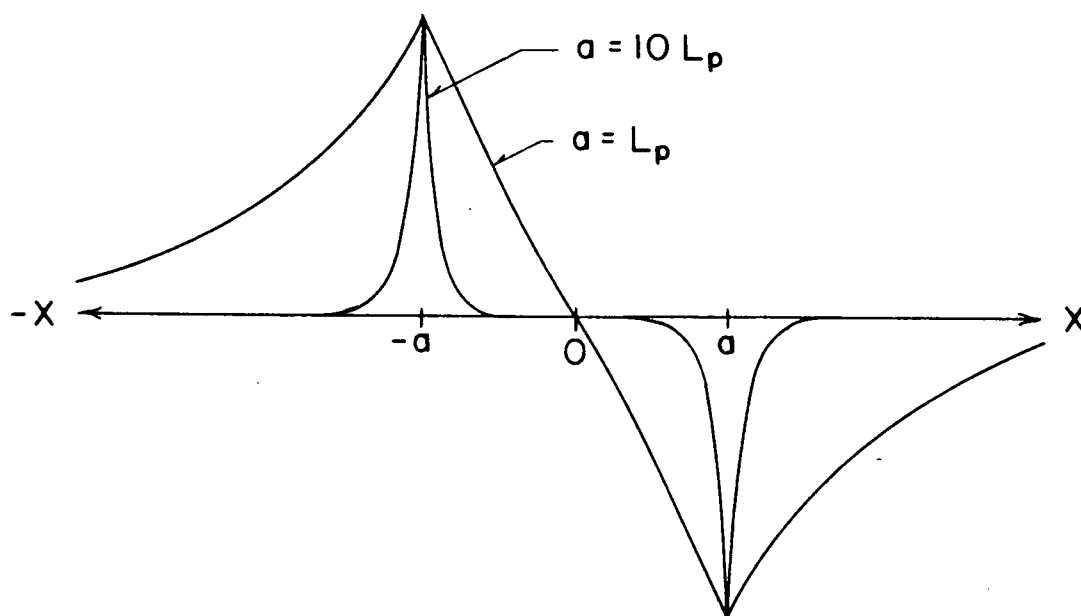
CARRIER CONCENTRATION GRADIENTS
(normalized)

Added carrier density and its gradient are
plotted in Figure 7 for $a \sim L_p$ and $a = 10 L_p$. Under
assumption (f) the gradient of added carrier density is
a delta function at the illumination edges, whereas
Figure 7 shows that in reality a significant gradient
of added carrier density exists over the smaller of $2 L_p$
or $L_p + a$ at each edge of illumination. The integral
may still be evaluated by the methods shown in Appendix
III, but the equilibrium densities in the integrand are
not those at the illumination edges, but are the weighted
average of the individual densities over the region of
significant grad Δn . Hence assumption (f) introduces
negligible errors if

$$L_a \left| grad \left(\ln n_o \right) \right| < 1$$

The above equations and Figure 7 show that a
significant added carrier concentration extends over the
illuminated region plus a diffusion length on either side,
i.e., over $2 \left(a + L_p \right)$. Since the bulk photo e.m.f. arises
from added carrier density and its gradient, the effectively
illuminated region extends a diffusion length beyond the
region where light is incident.

In the inner field term, the integral exists
over the region of significant added carrier concentration,
and the integral may be evaluated by the methods of Appendix

III if Δn_L is considered the average added carrier

density over the region of significant Δn . From these

considerations, the form of the bulk photo e.m.f.

expression derived under assumption (f) is approximately

valid even though the carrier distribution is quite

different from that implied by assumption (f). The bulk

photo e.m.f. is a function of the equilibrium conductivi-

ties at the edge of the region of significant Δn , and

the incident light may be considered an experimental

probe which samples the local conductivity variations.

Figure 7 illustrates that the minimum sampling diameter

with a vanishingly small illuminated region is two diffusion

lengths. Consequently if the bulk photo e.m.f. is used

to investigate crystal impurity gradients, it will show

only the variations which occur over the order of two

diffusion lengths. Finer variations in impurity may be

observed by decreasing the effective lifetime and diffusion

length, for instance by surface treatment, but this will

correspondingly decrease the net added carrier concentration

and photo e.m.f. at a given light intensity; it would

also make the recombination mechanism preponderantly signifi-

cant at the surface compared with the bulk, and the

photocarrier distribution would be markedly inhomogeneous

across the filament normal to the illuminated surface.

2.4 Photo e.m.f. at an Illuminated Junction

The photo e.m.f.'s arising from illumination of a bulk inhomogeneity and of a p-n junction represent two extremes of the same effect. However, the behaviour of the gradients of imrefs and electrostatic potential in the p-n junction differs from that in the bulk inhomogeneity. In the p-n junction the imref is the slowly varying quantity while the electrostatic potential has its maximum change in the transition layer. Electrical neutrality does not hold in this region and although

$$e = \int grad\ (\psi - \psi_0)\ dx$$

is valid, the approximate expression

$$grad(\psi - \psi_0) = \frac{kT}{q}\left[\frac{(b+1)\ grad\ \Delta n}{p_0 + bn_0 + (b+1)\Delta n} - \frac{(b+1)\Delta n\ grad\ n_0}{bn_0^2 + \Delta n(b+1)n_0 + n_i^2}\right]$$

used previously to derive the bulk photo e.m.f. is not applicable in the illuminated junction since it assumes $\Delta n = \Delta p$ and grad Δn = grad Δp .

The integral of the imref gradient can be evaluated to a close approximation however, since the change of imref is very nearly zero across the transition region (Fig. 3).

$$\int_a^b grad\ \phi_{n,p}\ dx = \int_a^{a'} + \int_{a'}^{b'} + \int_{b'}^b$$

and

$$\int_{a'}^{b'} \text{grad } \phi_{p,n} \, dx \doteq 0$$

where a and b are two unperturbed points in the p and n regions and a' and b' mark the edges of the transition layer. This approximation is used by Shockley (1949) in his analysis of the biassed p-n junction, and is also justified in the illuminated p-n junction.

Assuming the impurity density has an abrupt change of type at a given plane, the width of the transition layer W may be calculated and is characteristically of the order of 10^{-4} centimeters wide for impurity density to potential step ratio of $10^{15} \text{cm}^{-3} \text{v}^{-1}$. If the imref slope in the transition region approached $\frac{kT}{q L_a}$, the strong illumination maximum slope of the minority carrier imref, (see Appendix I), this would correspond to an imref change of no more than $\frac{kT W}{q L_a}$. The diffusion length L_a will ordinarily be of the order of 0.1 millimeters which is small compared to W, and thus $\frac{kT W}{q L_a}$ will be small compared with a typical weak illumination e.m.f. of $\frac{kT}{q}$ or more. In addition to this, the continuity equations show that the space derivatives of the carrier currents change sign at the edges of illumination, and the carrier currents are zero at one point inside the illuminated region (Figure 3). Consequently the imref slopes are smaller inside

the illuminated regions than at the edges, and if the illumination is confined to the transition layer the slopes are zero at one point inside it. These considerations show that the assumption of zero imref change across the transition region is well justified, and the p-n junction photo e.m.f. is

$$e_r = \int_a^{a'} grad\ \phi_{n,p}\ dx + \int_{b'}^{b} grad\ \phi_{n,p}\ dx$$

Assuming the p and n regions are homogeneous, the integral of the electron imref gradient gives (see Appendix IV),

$$e_r = -\frac{kT}{q}\ ln\ \frac{n_{op} + (\Delta n_L)_p}{n_{op}}\ \frac{n_{on}}{n_{on} + (\Delta n_L)_n}$$

$$+\ \frac{(b-1)}{(b+1)}\ \frac{kT}{q}\ ln\ \frac{1 + (b+1)(\Delta n_L)_p / p_{op} + b\, n_{op}}{1 + (b+1)(\Delta n_L)_n / p_{on} + b\, n_{on}}$$

Where subscript p and n refer to carrier densities in the p and n materials and Δn_L is the added carrier concentration at the edges of illumination, i.e., at the boundaries of the transition layer.

Integration of the hole imref between these same limits must give an identical expression for the photo e.m.f., and this provides a convenient check on the derivation. Using the hole imref

$$e_r = \frac{kT}{q} \ln \frac{p_{op} + (\Delta n_L)_p}{p_{op}} \frac{p_{on}}{p_{on} + (\Delta n_L)_n}$$

$$+ \frac{(b-1)}{(b+1)} \frac{kT}{q} \ln \frac{1 + (b+1)(\Delta n_L)_p / p_{op} + b n_{op}}{1 + (b+1)(\Delta n_L)_n / p_{on} + b n_{on}}$$

Since the two expressions have the same second term, the first terms must be equal, and this can be shown to follow from the assumption of zero imref change across the transition layer. When the imref change is zero, the differences of imrefs are equal at the transition boundaries, i.e.,

$$\left(\phi_p - \phi_n\right)_n = \left(\phi_p - \phi_n\right)_p$$

But

$$\left(\phi_p - \phi_n\right)_n = \frac{kT}{q} \ln \frac{n_n p_n}{n_i^2}$$

$$\left(\phi_p - \phi_n\right)_p = \frac{kT}{q} \ln \frac{n_p p_p}{n_i^2}$$

where n_n, p_n and n_p, p_p are the carrier concentrations at the boundaries of the transition layer.

Thus

$$\frac{kT}{q} \ln \frac{p_p n_p}{p_n n_n} = 0$$

or

$$\frac{kT}{q} \ln \frac{p_{op} + (\Delta n_L)_p}{p_{on} + (\Delta n_L)_n} = -\frac{kT}{q} \ln \frac{n_{op} + (\Delta n_L)_p}{n_{on} + (\Delta n_L)_n}$$

and since $\dfrac{n_{on}}{n_{op}} = \dfrac{p_{op}}{p_{on}}$

the first terms of the two expressions for the e.m.f. are
equal.

If the carrier lifetimes are substantially
different in the p and n regions the imrefs will tend to
separate less in the region of low lifetime. This produces
a sharp gradient of imrefs across the transition layer
which corresponds to a large flux of carriers of both signs
into the low lifetime side, maintaining the separation of
the imrefs essentially equal at both edges of the transi-
tion layer. Thus the relative magnitudes of the carrier
concentrations $\left(\Delta n_L\right)_n$ and $\left(\Delta n_L\right)_p$ are insensitive to lifetime
and are dependent on the equilibrium majority carrier
densities in the material on either side of the junction
(see Appendix VI).

The above expressions for photo e.m.f. were derived
with no restrictions as to the type of material on either
side of the junctions, and can be applied to any type of
junction where zero imref change across the transition layer
may be assumed. It should be noted that zero imref change
has been used to imply equal differences of imrefs at the
transition boundaries, which is a less restrictive condition,
and the derivation will be valid so long as the imref
changes across the transition layer are equal or zero.

With weak illumination the added carrier densities
are negligible compared with the equilibrium majority carrier

densities, and the p-n junction photo e.m.f. becomes

$$e_r = -\frac{kT}{q} \ln\left[1 + \frac{(\Delta n_L)_p}{n_{op}}\right] = -\frac{kT}{q} \ln\left[1 + \frac{(\Delta n_L)_n}{p_{on}}\right]$$

and the photo e.m.f. is proportional to log light intensity when (Δn_L) lies between the majority and minority carrier densities. At strong illumination the photo e.m.f. saturates to

$$e_r = -\frac{kT}{q} \ln\frac{n_{on}}{n_{op}} + \frac{(b-1)}{(b+1)} \frac{kT}{q} \frac{p_{on} + b n_{on}}{p_{op} + b n_{op}}$$

$$= -\left(\psi_{on} - \psi_{op}\right) + \frac{(b-1)}{(b+1)} \frac{kT}{q} \ln\frac{\sigma_{on}}{\sigma_{op}}$$

The second term of the saturation e.m.f. involves the log of the ratios of conductivities of the material on either side of the junction, and will ordinarily be small compared with the first term. The saturation e.m.f. is then approximately equal to the equilibrium electrostatic potential step at the junction.

The weak illumination photo e.m.f. in a n-n+ junction becomes

$$e_r = -\frac{kT}{qb}\left(\Delta n_L\right)_n \frac{1}{n_{on}}$$

which is equivalent to the result obtained from illumination of a bulk inhomogeneity (see section 2.3) when $n_{on+} \gg n_{on}$.

These expressions for the photo e.m.f. at illuminated junctions hold for an arbitrary concentration of photo generated carriers. The form of the e.m.f. expression is the same as that derived by Cummerow (1954) for very weak

illumination $\left(\Delta n_{L} \ll n_{op}, p_{on} \right)$ where the e.m.f. is
proportional to light intensity, and for weak illumination
$\left(n_{op} < \Delta n_{L} < p_{op} \right)$ where the e.m.f. is proportional to
log light intensity. Cummerow's treatment however, does not
show saturation e.m.f. at strong illumination.

In a p-n junction, the second term of the e.m.f.
expression will be very small since the conductivities of
the p and n materials will ordinarily be of the same order
of magnitude. In this case the only significant contribution
to the e.m.f. arises from the first term, which is identical
with an expression derived by Fan (1948).

2.5 Bulk Photo e.m.f. in a Near Intrinsic Semiconductor

Assuming complete impurity ionization and electrical neutrality, the equilibrium carrier densities in a semiconductor may be written in terms of intrinsic carrier concentration, n_i, and the net positive impurity ion density, N_D-N_A (see section 1.1).

$$n_o = \frac{N_D - N_A}{2} + \sqrt{\left[\frac{N_D - N_A}{2}\right]^2 + n_i^2}$$

$$p_o = -\frac{N_D - N_A}{2} + \sqrt{\left[\frac{N_D - N_A}{2}\right]^2 + n_i^2}$$

We consider a semiconductor to be near intrinsic when $n_i >> \left|N_D - N_A\right|$, and in this case the equilibrium carrier concentrations are approximately

$$n_o = \frac{N_D - N_A}{2} + n_i$$

$$p_o = -\frac{N_D - N_A}{2} + n_i$$

The analysis of the bulk photo e.m.f. in section 2.3 gives a general expression for the e.m.f. in terms of the added carrier concentration in the illuminated region and the equilibrium carrier concentrations at the edges. The e.m.f. in near intrinsic material is obtained by substituting the above carrier densities into the general expression. If the semiconductor is illuminated between points a' and b' and

assumptions (a) to (g) used in the general treatment are valid, the e.m.f. between unperturbed points a and b is

$$e_B = -\frac{2b}{(b+1)^2} \frac{kT}{q} \Delta n_L \frac{(N_D - N_A)_{b'} - (N_D - N_A)_{a'}}{n_i^2}$$

for weak illumination $\left(\Delta n_L \ll n_i\right)$

and

$$e_B = -\frac{2b}{(b+1)^2} \frac{kT}{q} \frac{(N_D - N_A)_{b'} - (N_D - N_A)_{a'}}{n_i}$$

for strong illumination $\left(\Delta n_L \gg n_i\right)$

2.6 Ratio of Bulk Photo e.m.f. to Photoconductive Decrease of Resistance

Illumination of a semiconductor filament increases the number of carriers available for conduction and thus decreases the filament resistance. In the following this photo conductive resistance decrease ΔR will be referred to as the photo resistance, and is equal to the filament resistance in the dark minus the illuminated resistance. If the illuminated region has an impurity gradient, the added carrier density will also give rise to a bulk photo e.m.f. Both these effects originate from the same carrier distribution and their ratio does not contain the added carrier density. This gives a convenient method of relating the bulk photo e.m.f. to the semiconductor impurity gradient without knowledge of the illumination intensity in terms of the number of effective photons absorbed per second.

For weak illumination, the bulk photo e.m.f. in an n-type semiconductor may be written (see section 2.3)

$$e_B = \frac{2\,kT}{q\,b}\ \Delta n_L \left[\frac{1}{n_{ob'}} - \frac{1}{n_{oa'}} \right]$$

where Δn_L is the added carrier concentration in the illuminated region, and $n_{ob'}$ and $n_{oa'}$ are the equilibrium carrier densities at the illumination edges.

When the filament is uniformly illuminated producing a constant added carrier density throughout the volume under

the illuminated area,

$$\Delta R = R_0 - \frac{1}{A} \int_L \frac{dx}{\sigma_0 + \Delta\sigma}$$

where R_0 is the equilibrium dark resistance, A is the crossectional area, and the integration is over the entire length, L, of the filament. $\Delta\sigma$, the conductivity increase due to illumination, is assumed small compared with σ_0 , the equilibrium conductivity. Thus

$$\Delta R = \frac{q}{A}(\mu_n + \mu_p)\Delta n_L \int_{a'}^{b'} \frac{dx}{\sigma_{0_L}^2}$$

The integration limits are the edges of illumination since Δn_L is zero elsewhere and σ_0^2 becomes $\sigma_{0_L}^2$, the average equilibrium conductivity over the illuminated region. The ratio of bulk photo e.m.f. to photo resistance becomes,

$$\frac{e_B}{\Delta R} = \frac{2A}{b+1} \frac{kT}{q} \frac{\sigma_{0a'} - \sigma_{b'}}{b' - a'}$$

The illuminated region acts as an experimental probe which samples the equilibrium conductivities at the illumination edges a' and b' (see section 2.3). If the illuminated region is sufficiently narrow that the equilibrium conductivity fluctuations may be regarded as monotonic within it, then the ratio is approximately

$$\frac{e_B}{\Delta R} = -\frac{2A}{b+1} \frac{kT}{q} \frac{d\sigma_0}{dx}$$

In impurity semiconductors the conductivity is very closely
proportional to the impurity density, and the bulk photo
e.m.f. may be expressed in terms of the conductivity
gradient. However, conductivity has a minimum where

$$N_D - N_A = \frac{1 - b}{n_i \sqrt{b}}$$

and in near intrinsic material the ratio of bulk photo e.m.f.
to photo resistance must be expressed in terms of the
impurity density gradient. Using the approximations and
results of section 2.5

$$\frac{e_B}{\Delta R} = \frac{2 k T A b}{\mu_p (b+1)} \frac{d}{dx} \left(N_D - N_A \right)$$

The ratio of bulk photo voltage to photo resis-
tance was derived assuming a uniform added carrier density
throughout the volume under the illuminated area, and this
brings the filament crossectional area into the expression
for photo resistance. Consequently, when the ratio is
used to estimate the conductivity gradient, the condition
of uniform added carrier density must be closely approxi-
mated. With a non-uniform added carrier concentration,
the effective crossectional area is unknown and a
quantitative estimate of the conductivity gradient cannot
be obtained. The photo resistance is linear with light
intensity for weak illumination $\Delta \sigma << \sigma_0$. As the
light intensity is increased the illuminated region approaches
zero resistance and the increase in the photo resistance
is predominantly due to carrier diffusion away from the

illumination edges. As a result the photo resistance is
proportional to log light intensity with strong illumina-
tion since the photo resistance there depends chiefly
on diffusional spread of carriers and is insensitive to
impurity gradients.

The bulk photo e.m.f. is linear with light intensity
for weak illumination. However, at strong illumination,
the e.m.f. component in the illuminated region may reach
saturation, and if the added carrier density is increased
further, any e.m.f. change must arise from carriers that
have diffused far enough to arrive in an unsaturated region.
This has the effect of increasing the region of significant
added carrier concentration beyond $2(a + L_a)$ (see section
2.3). If the region outside the area of illumination has
a resistivity gradient opposite to that in the illuminated
region, the net effect is a lowering of the observed
"saturation" e.m.f. On the other hand, if the impurity
gradient increases monotonically along the filament, the
strong illumination increase of the region of significant
added carrier concentration will give rise to e.m.f.
components of the same polarity as the saturated component,
and the bulk photo e.m.f. will increase monotonically with
strong illumination. In the first case, the behaviour
of the strong illumination photo e.m.f. is unlike the photo
resistance behaviour and the ratio of these quantities is
constant at weak illumination only. In the second case,
the photo e.m.f. increase with strong illumination depends

entirely on diffusional carrier spreading, and the ratio
of photo e.m.f. to photo resistance is constant at all
light intensities.

C H A P T E R   I I I - P R E P A R A T O R Y
E X P E R I M E N T S

3.1 Filament Preparation

The germanium filaments used for photo e.m.f.
observations were cut from monocrystalline ingots using a
reciprocating wire saw. Typical filaments had a rectangular
crossection of $\sim 1mm^2$ and a length of $\sim 1.5\,cm$. After
the filaments were cut and cleaned, the ends were sandblasted
and electroplated to obtain a metallic contact to the material
(see section 3.2). The filament was then heated in an inert
atmosphere, tin was melted on the plated areas and 0.010 inch
diameter wire leads were attached. The filaments were mounted
by securing the leads in phosphor bronze clips which were
bolted on a plastic holder. The clips served as terminals by
which the filament was connected to the measuring circuits.

If the photo e.m.f. is used to investigate satura-
tion photo effects, a long carrier lifetime is desirable,
while investigation of filament conductivity variations
requires a short lifetime and carrier diffusion length
(section 2.3). With a $1mm^2$ crossection, the effective carrier
lifetime in the filaments was strongly dependent on surface
conditions through the surface recombination velocity. The
filament effective decay constant (reciprocal of lifetime) is
the sum of a bulk and a surface decay constant (Shockley 1950).

$$\nu_f = \nu_B + \nu_s$$

$$\text{and} \quad \nu_s = \frac{\pi^2 D_a}{4}\left[\frac{1}{B^2} + \frac{1}{C^2}\right] \qquad s \to \infty$$

$$= s\left[\frac{1}{B} + \frac{1}{C}\right] \qquad s \to 0$$

where s is the surface recombination velocity (cm./sec.),
2B and 2C are the crossectional dimensions of the filament
and D_a is ambipolar diffusivity. High surface recombination
velocity and short effective lifetimes were obtained by
sandblasting or polishing the filament surfaces and the
surface recombination velocity was reduced by etching the
filament in a 3% solution of hydrogen peroxide. Hydrogen
peroxide has the advantage of being easier to handle than
the fluoride etchants, and does not attack the metallic
contacts.

3.2 Metal-Semiconductor Contacts

Metal to semiconductor contacts in general show some degree of rectification depending on the method of contact fabrication. When an n-semiconductor filament is heated and a metal wire alloyed with an acceptor element melted onto it, a p-n junction is formed at the contact. If the wire is alloyed with a donor element, a low-high (L-H) n-n+ junction is formed. The p-n junction is unsuitable as a contact since its reverse resistance is ordinarily large compared with a typical filament resistance and because it is photo sensitive and can cause injection effects. The L-H junction has negligible resistance for both directions of current flow and provides an electrically "smooth" metal to extrinsic semiconductor transition. The alloying technique however, is not particularly successful in contacts too near intrinsic material.

In this work we were not primarily concerned with the characteristics of metal to semiconductor contacts, which were considered acceptable if their resistance change with a moderate current density increase was small compared with the resistance of filament plus contact. A one per cent overall resistance change with a current density of plus or minus one amp/cm^2 was chosen as a tolerable upper limit of non-ohmic behaviour, and an attempt was made to achieve this figure by using soldered or electroplated contacts.

DEPENDENCE OF FILAMENT PLUS CONTACT RESISTANCE

ON CURRENT DENSITY
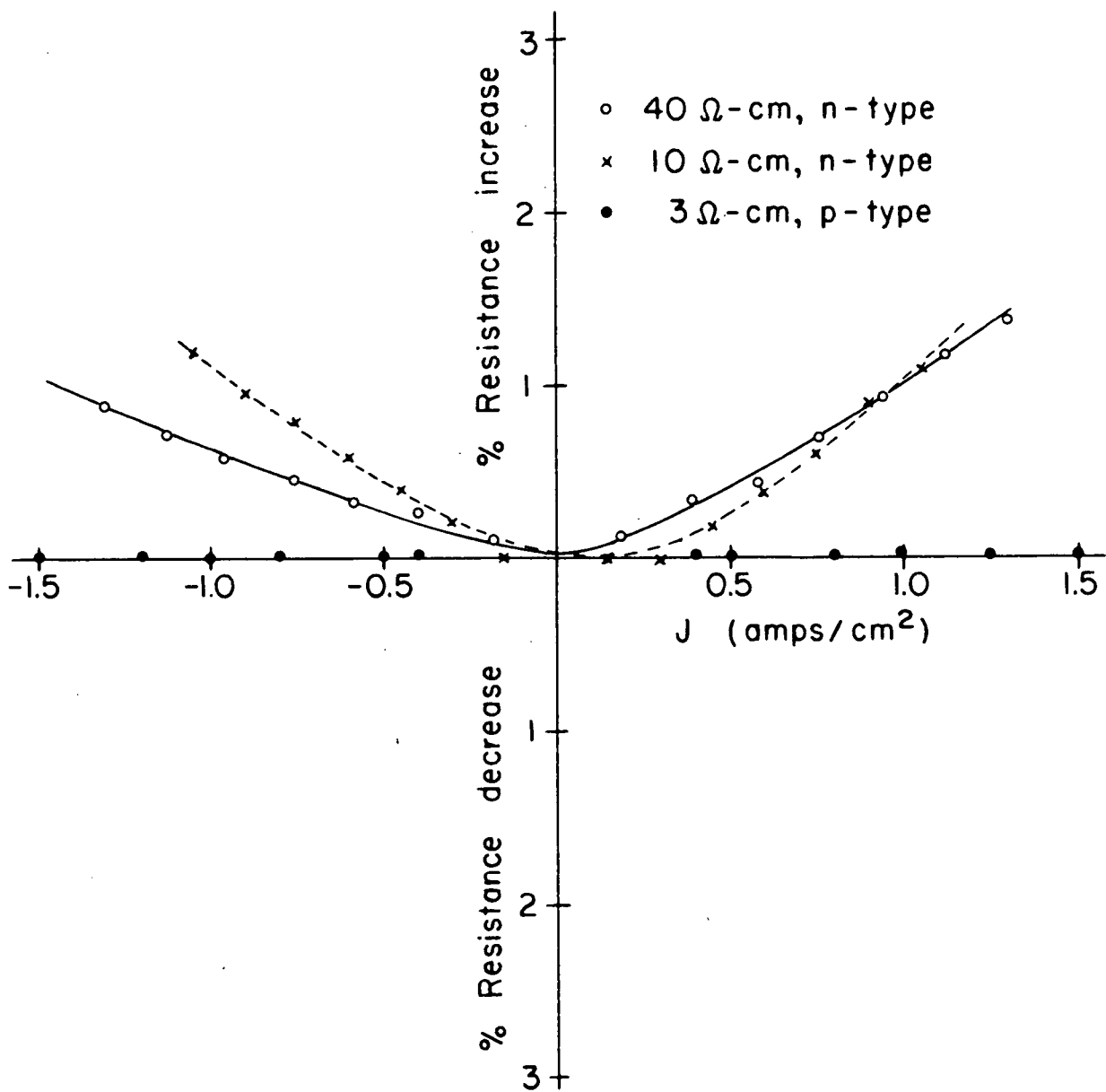
Each solder or electroplate was given two trials, once on a sandblasted, and on an etched surface since these correspond to the two extremes of surface condition at the contact. The soldering trials were made using pure tin, pure lead, antimony-doped tin, antimony-doped lead, and both pure and doped 50-50 solder. These contacts gave non-ohmic behaviour which ranged from five to twenty per cent resistance change with one amp./cm.^{2} current density increase.

Plated contacts gave more satisfactory results. Nickel, copper and rhodium plating was tried, with various temperatures, plating current densities and Ge surface conditions. Optimum contact characteristics were obtained using a rhodium plate (Weisberg 1953) on a sandblasted surface at room temperature and 20 ma/cm.^{2} plating current density. This gave a resistance change of one to two per cent at 1 amp./cm.^{2} with the n-type and near intrinsic materials (Fig. 8). With the 3 ohm-cm p-type, rhodium plate on a sandblasted surface gave less than 0.2% resistance change up to 15 amp./cm.^{2}. Plating on etched surfaces gave markedly non-ohmic contact with n and near-intrinsic material, but in the p-type was not noticeably different from results obtained by plating over a sand blasted surface. These observations are in agreement with those of Borneman (1955). The conductivity of germanium in the intrinsic range is a rapidly increasing function of temperature, and with the near intrinsic filaments at room temperature, as much as five per cent filament resistance change could result from one degree Centigrade

temperature change. Hence the measurements of contact
linearity were made with an ambient temperature constant
to better than 0.1 degrees Centigrade and to avoid electri-
cal heating the filament resistance was measured on a
wheatstone bridge using 60μ sec. pulses at a 30 pps repeti-
tion rate as the bridge current source. The bridge balance
point was obtained using an oscilloscope with a differential
input amplifier. The departure from linearity of the
resistance versus current density plot indicated the
quality of the contact; if the variation was symmetrical
the indication was that the contacts were electrically
equivalent and would be reproducible. When asymmetry was
observed, the implication was that the contacts under study
would not be closely reproducible.

Plated Cu_3Ge (Fink 1948) was also given a trial
as a contact to germanium filaments. This compound has the
electrical characteristics of a metal, and gives a bright
silver coloured deposit that is inert to concentrated nitric
or sulphuric acid. In this respect its chemical properties
are similar to germanium. Considering the characteristics
of this material it seemed plausible that it might provide
a smooth electrical transition from metal to semiconductor.
The electrical characteristics of the plated contacts of Cu_3Ge
were acceptable but not better than the rhodium contacts.
In the course of a few months the Cu_3Ge plated on germanium
lost its lustre and darkened, while a deposit on a metal
backing remained bright and untarnished. This behaviour was a
further reason for rejecting the compound as a contact material.

3.3 Filament Conductivities

A semiconductor in the intrinsic range has an equal number of carriers of both signs, and the conductivity is

$$\sigma = q \, n_i \left(\mu_n + \mu_p \right)$$

The intrinsic concentration n_i and the mobilities are both temperature dependent. In germanium at temperatures from $100°K$ to $500°K$ the electron mobility is proportional to $T^{-1.66}$ and the hole mobility to $T^{-2.33}$ (Morin 1954). The variation of these quantities with temperatures is slow compared with that of the intrinsic concentration

$$n_i \propto T^{3/2} \exp - \frac{E_g}{2kT}$$

and thus to a close approximation

$$\sigma = C \exp - \frac{E_g}{2kT}$$

A plot of log σ versus $1/T$ gives a straight line in the intrinsic range of conductivity, from which the energy gap at absolute zero, E_g, is determined. At lower temperatures, the intrinsic concentration becomes negligible compared with carriers arising from impurity centers, and if the impurities may be assumed totally ionized (see section 1.1) the conductivities are

$$\sigma = q \mu_n \left(N_D - N_A \right) \qquad \text{in n-type}$$

$$\sigma = q \mu_p \left(N_A - N_D \right) \qquad \text{in p-type}$$

FIGURE 9

CONDUCTIVITY TEMPERATURE DEPENDENCE

OF THE GERMANIUM FILAMENTS
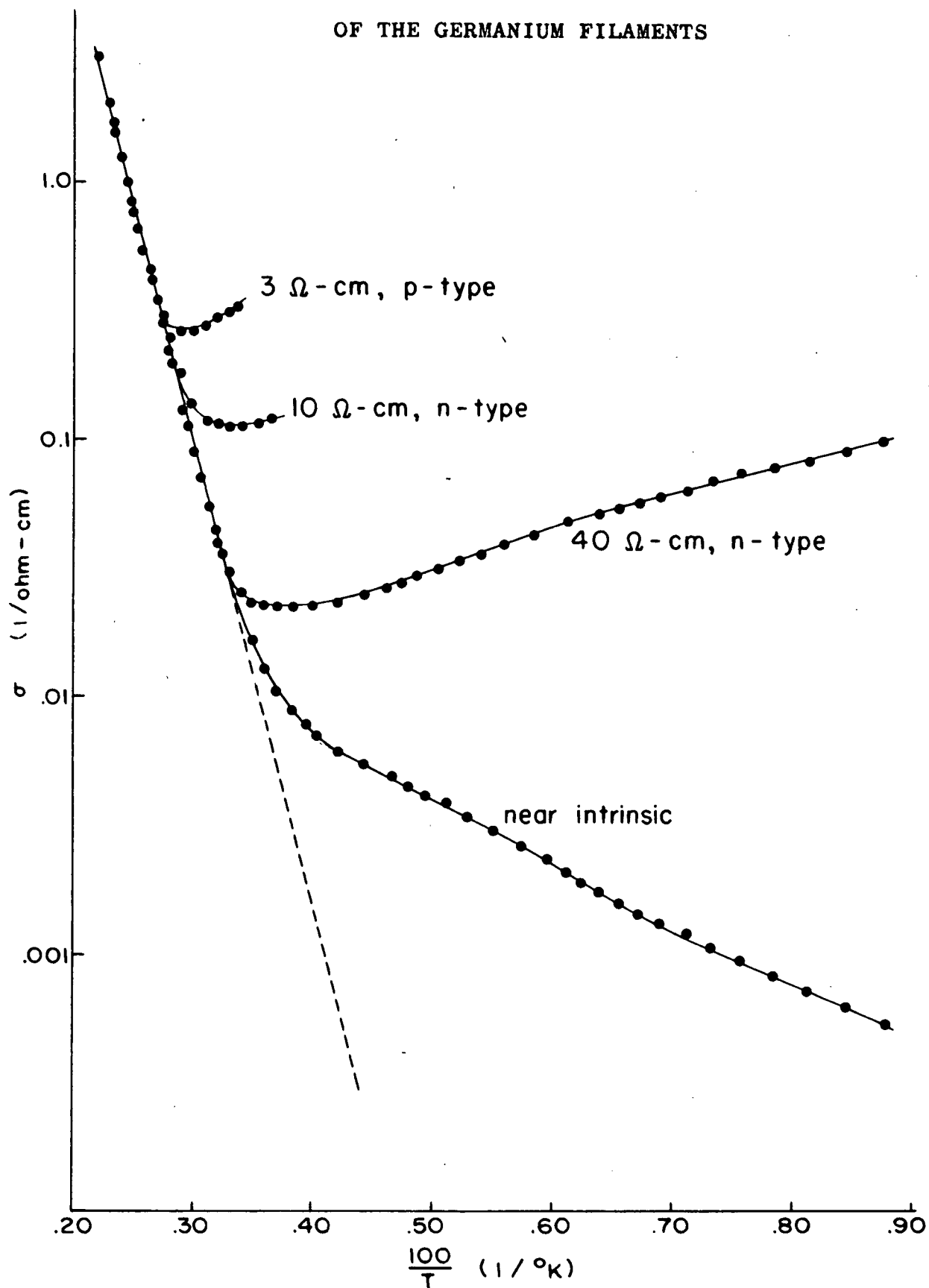
Using published data on mobility these extrinsic conductivities give an estimate of (N_D - N_A).

The germanium filaments used in this work were cut from ingots of 3 ohm-cm p-type, 10 and 40 ohm-cm n-type, and from a near intrinsic ingot with residual n impurities. Filaments were also taken from a "graded" n ingot having a monotonic resistivity gradient from approximately 3 ohm-cm to 30 ohm-cm over a 5 cm. length. The conductivity temperature dependence of these materials are plotted in Figure 9. The graded specimen is not included because of its extreme inhomogeneity. The filaments were glued in turn to a thermometer bulb and heated in an oil bath to 150°C. Resistance and temperature readings were taken simultaneously as the bath cooled to room temperature. For low temperatures a copper-constantan thermocouple was attached to one terminal of the filament. The filament was immersed in petroleum ether cooled to liquid nitrogen temperature and resistance and temperature readings were taken simultaneously as the bath warmed to room temperature. With this relatively simple experimental set-up, the values of energy gap obtained were close to the accepted value of 0.785 ev. (Morin 1954) and this leads us to place considerable confidence in our values of (N_D - N_A).

Table   I

Material	Resistivity at 20°C (ohm-cm)	Apparent Eg (ev)	$(N_D - N_A)$ (cm^{-3})
p	3.1	0.783	1.14×10^{15}
n	9.1	0.725	1.75×10^{14}
n	40.0	0.750	2.87×10^{13}
near intrinsic	56.0		approx. 10^{13}

Close agreement with the accepted value of germanium zero-temperature energy gap was obtained with the p specimen confirming the ohmic quality of the contacts to this material.

SPECTRAL DISTRIBUTION OF RADIATION FROM A

ZIRCONIUM CONCENTRATED-ARC LAMP

2590

1800

1600

1400

1200

1000

WATTS/CM^2

800

600

400

WAVELENGH IN MICRONS

200

0.3   0.4   0.5   0.6   0.7   0.8   0.9   1.0
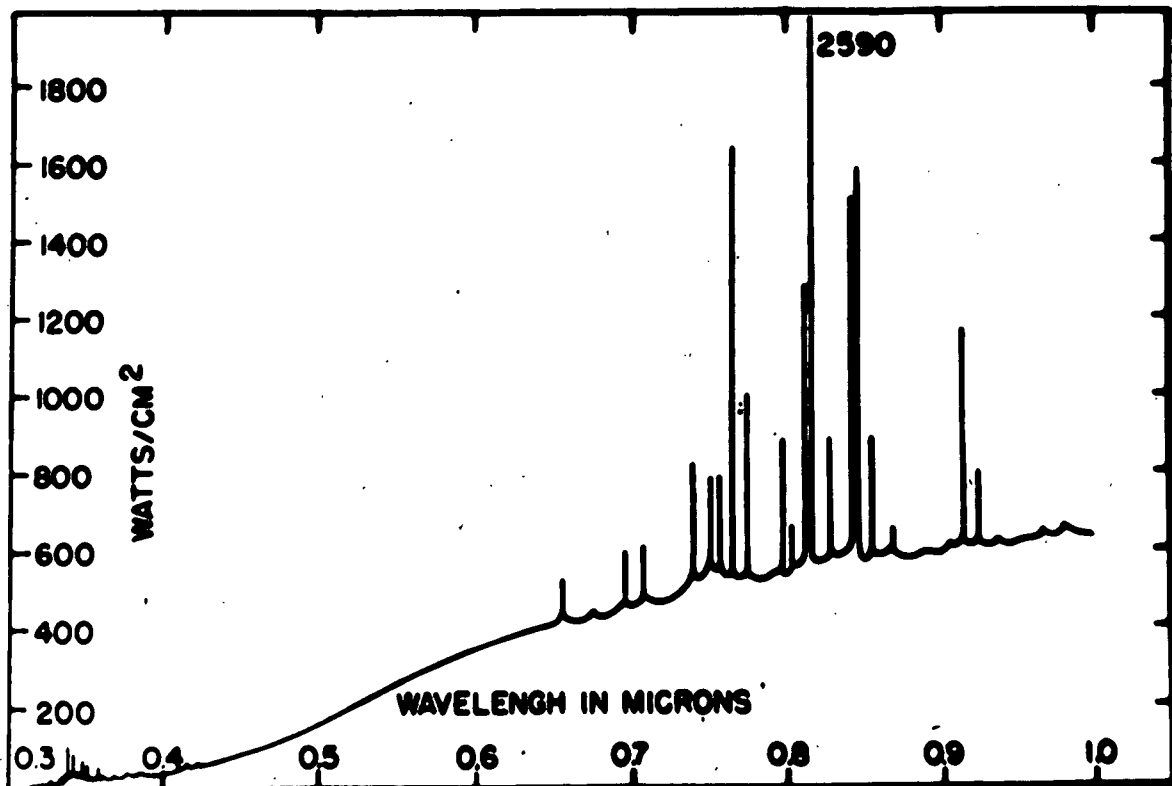
3.4 Apparatus

When a germanium filament is illuminated with a
small light spot in a region of impurity density gradient,
a bulk photo e.m.f. is observed between the end contacts.
If the spot is scanned over the length of the filament and
the voltage plotted as a function of position, the e.m.f.
pattern obtained is characteristic of the filament and is
related to its impurity distribution.

Two light sources, a one hundred watt "Point-o-Lite",
and a twenty-five watt zirconium arc lamp were used for
developing the bulk photo e.m.f. The point-o-lite is
essentially a black body radiator while the zirconium arc
has a continuous spectrum and many very intense lines. The
spectral distribution of the zirconium arc as supplied by the
manufacturer is shown in Figure 10. The zirconium arc was
a more intense source than the point-o-lite, and was used for
most of the photo e.m.f. work. Both sources produced intense
spots of approximately 0.1 inch diameter with the Point-o-
Lite, and 0.03 inch diameter with the zirconium arc. These
were demagnified using a two lens system to 0.1 millimeter
diameter or larger at the germanium filament surface.

The filament on its plastic holder was bolted to
a small carriage which moved vertically in a brass track,
and the second lens of the optical system was mounted rigidly
in front of it (Figure 11). Adjusting screws were provided
so that the carriage and track could be moved in a horizontal
plane parallel or perpendicular to the direction of the

FIGURE 11

SCANNING MECHANISM AND FILAMENT HOLDER
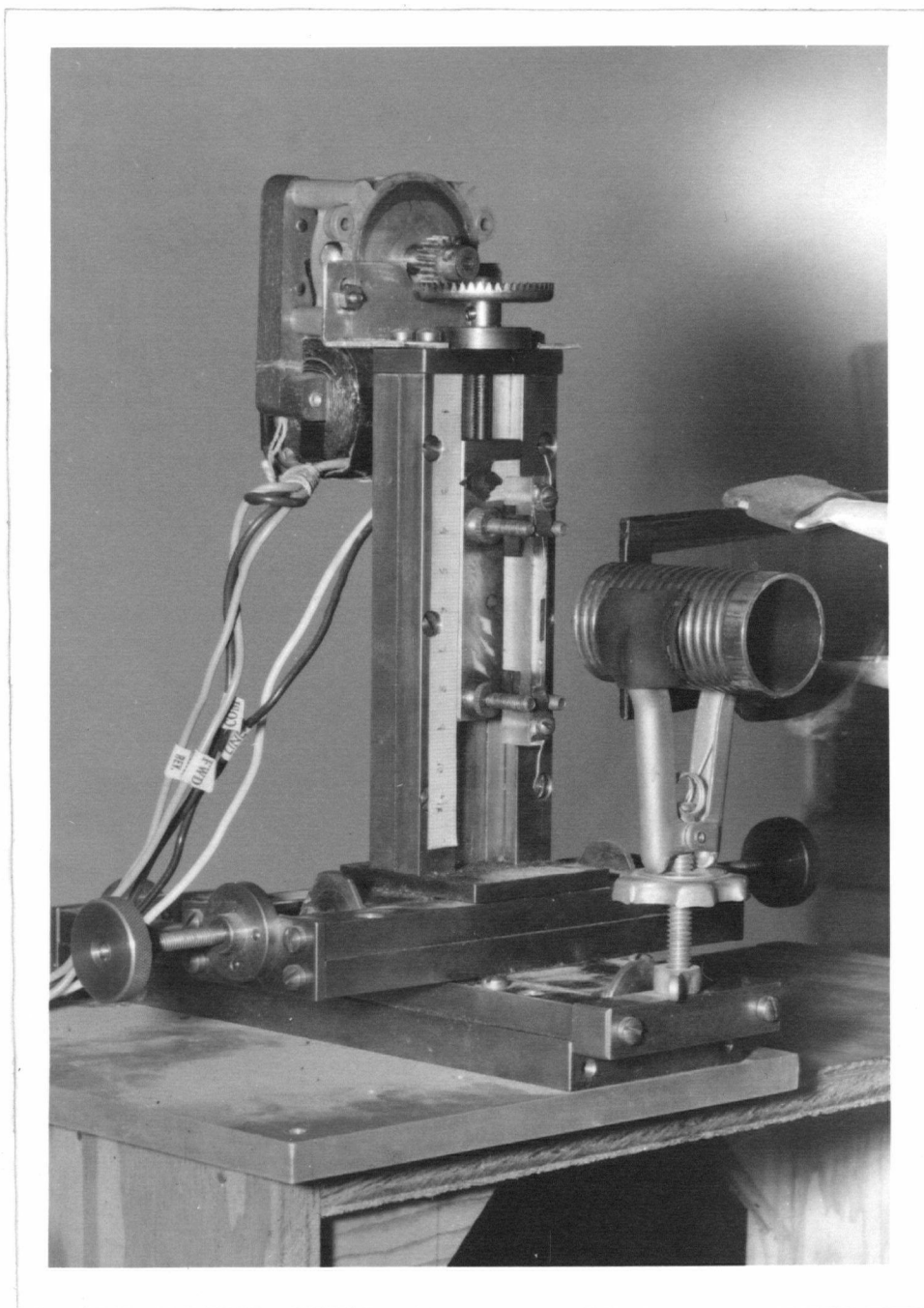
light. These were used to position and focus the light
spot on the filament. The carriage was driven by a reversible
synchronous clock motor, and the e.m.f. was recorded on a
0-10 mv recording potentiometer as the light spot scanned
the filament. Typical e.m.f. patterns obtained in this way
are reproduced in Figure 12, section 3.5.

For scanning at temperatures higher than room
temperature the whole assembly was placed in an insulated
box and the light beam was brought in through a lucite window.
The temperature inside the box was maintained constant within
1°C using an electronic thermal regulator. With this
arrangement the change of e.m.f. pattern with temperature
was observed up to 70°C.

DEPENDENCE OF BULK PHOTO E.M.F. PATTERNS

ON FILAMENT SURFACE CONDITIONS

POLISHED SURFACE

HEAVILY ETCHED SURFACE
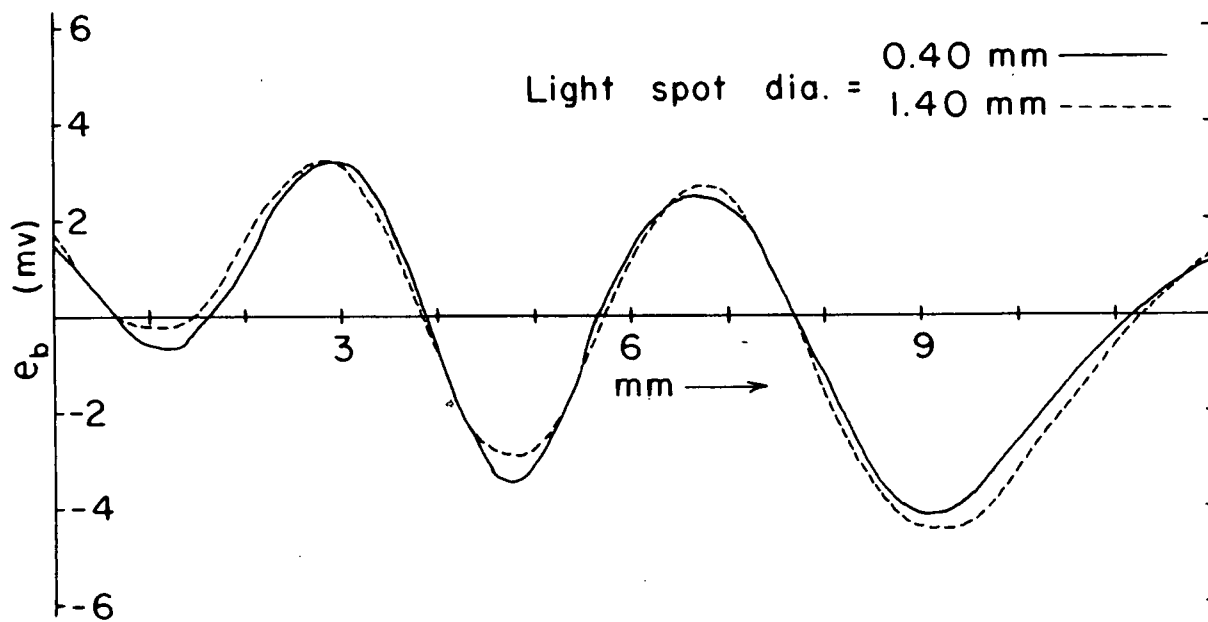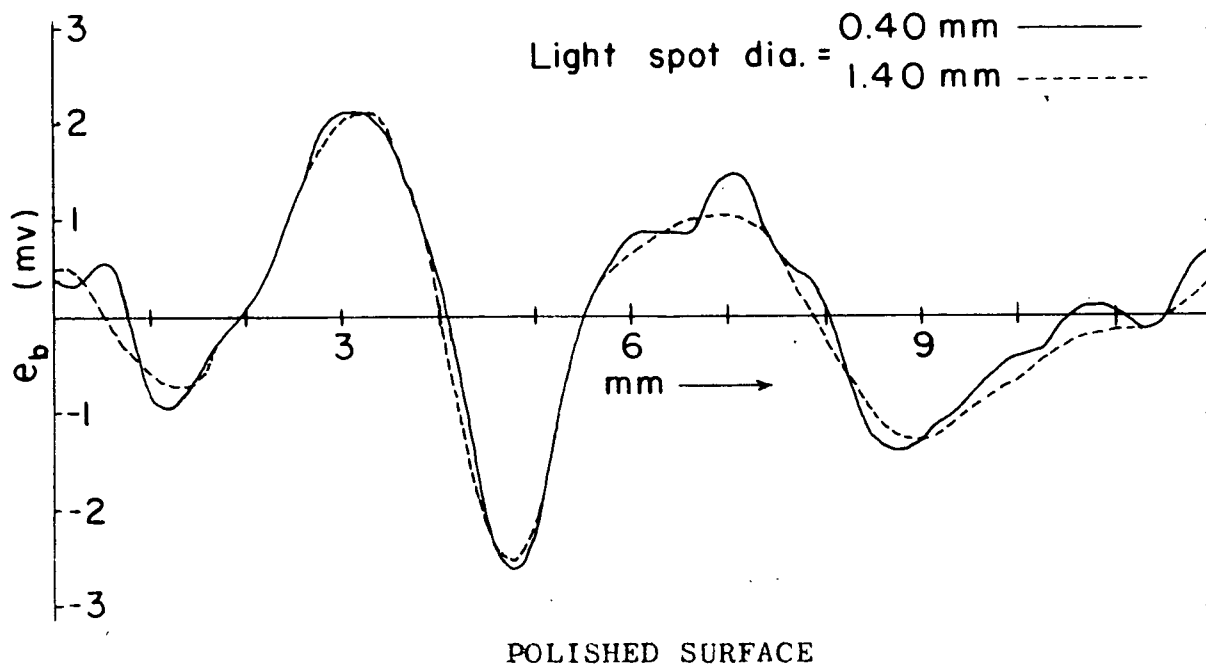
3.5 Identification of the Photo e.m.f. as a Bulk Effect

The magnitude and pattern of the positional variation of the photo e.m.f. observed with a given filament changed markedly with different surface conditions. This suggested the possibility that in some cases the observed photo e.m.f. originated from surface rather than bulk irregularities.

To identify the origin of the effect, the photo e.m.f. was examined as a function of illuminating position with surface conditions varying from the extremes of sand-blasted (high recombination velocity) to heavily etched (low recombination velocity). A light spot was scanned along a five centimeter long specimen and positional variation of photo e.m.f. was recorded. Three photo e.m.f. plots were made for each surface condition using light spot diameters of approximately 0.40, 0.80 and 1.40 millimeters. Surface conditions investigated were, in order, polished, sandblasted, and etched. The filament was subjected to four successive etches of four minutes in three per cent hydrogen peroxide at 45°C. and was scanned after each etch. Photo e.m.f. plots are shown in Figure 12 for the two extremes of surface conditions. The e.m.f. pattern observed with a polished surface showed many small peaks superimposed on larger peaks. As the light spot diameter was increased these smaller peaks were no longer resolved and the pattern reduced to several relatively broad peaks. The sandblasted surface showed

essentially the same patterns but with reduced amplitudes. All major e.m.f. peaks were in the same position.

The first three etches produced a progressive de-emphasis of the minor peaks with the smallest light spot diameter and after the third etch, the light spot diameter had very little effect on the photo e.m.f. pattern. The fourth etch produced no appreciable change in the e.m.f. pattern, indicating that the surface had reached the limiting condition obtainable with a hydrogen peroxide treatment. Throughout the entire range of surface conditions, the positions of the major peaks were unchanged.

Surface etching increases the carrier lifetime and diffusion length, and consequently increases the effective light spot diameter, i.e. diameter of the region of significant added carrier concentration. The effective light spot diameter can never be smaller than twice the diffusion length (see section 2.3) and this explains the insensitivity of photo e.m.f. to light spot diameter with the heavily etched surfaces. The disappearance of the smaller peaks when the surface is etched is also explained by the increase in the diameter of the region of significant added carrier concentration. As the sampling width increases only the grosser variations in impurity density are detected and the fine structure is averaged out. This explanation of the e.m.f. pattern change is borne out by the polished and sandblasted surfaces where carrier diffusion length is much shorter, and the effective light spot diameter approaches the actual

light spot diameter. In these cases the e.m.f. plot with
small light spot diameter is superficially dissimilar to
the etched surface plot while the pattern with large diameter
spot is very similar to it (Figure 12).

On the basis of these observations we may definitely
identify the observed photo e.m.f. as a bulk effect, and
consider surface conditions as one parameter determining
the dimensions of the sampling light probe. This conclusion
is supported by e.m.f. patterns obtained by scanning the four
sides of a filament. These were essentially the same even
with a polished surface. It was unlikely that surface
irregularities were the same on all sides of the filament,
and thus the similarity of the patterns indicate that the
observed e.m.f. originated from variations in the bulk
of the filament.

3.6 Measurement of Carrier Lifetimes

In a semiconductor in equilibrium, the volume rate of thermal generation of electron-hole pairs is exactly balanced by an equal volume rate of recombination. If excess carrier pairs are momentarily generated by some means, their effective lifetime τ is defined by

$$\frac{1}{\tau} = - \frac{1}{p - p_o} \frac{dp}{dt}$$

When the excess concentration is small compared with the equilibrium concentration, τ is the time required for the excess concentration to decay by a factor e^{-1}. Decay constants are defined as reciprocals of lifetimes.

The experimental arrangement for observation of effective lifetime is as follows. The germanium filament in series with a variable resistance is connected across a constant voltage source. A pulse of light generates excess carrier pairs in the germanium and the resulting increase of conductance causes a voltage increase at the resistor terminals which decays back to the steady state voltage as the photo-generated carrier pairs recombine. The time dependence of the photo-conductive voltage pulse across the resistor is the same as that of the excess carrier concentration provided that (i) no carriers are swept out of the filament (ii) filament surface conditions, bulk lifetime, and conductivity are uniform, (iii) no excess carrier generation occurs during the time of observation.

When the illumination consists of a light spot,

condition (i) is satisfied if the field conforms to the
sweep-out condition

$$F < \frac{d}{\mu_a \tau}$$

where d is the distance from the light spot to the contact
towards which the carriers are moving. If the whole filament
is illuminated, carriers will be swept out unless the field
is small enough that carrier motion is predominantly
diffusional

i.e. $$F < \frac{kT}{qL_a}$$

where $L_a = \sqrt{D_a \tau}$ is the ambipolar diffusion length. With
light spot illumination the field may cause appreciable drift
without violating the sweep-out condition. In this case
condition (ii), uniform surface conditions and bulk lifetime
must apply, for otherwise the recombination rate changes
as the carriers move along the filament. The effects of non-
uniform conductivity are discussed in section 3.7. If
surface and bulk conditions are not uniform, the field must
be reduced to conform with the diffusional condition, and
the photo-conductive pulse gives a measure of the carrier
lifetime at the point of illumination. The measured effective
decay constant may be considered the sum of a bulk and a
surface decay constant (section 3.1) and by measuring decay
constants under the extremes of high and low surface
recombination velocity, a measure of the bulk lifetime can
be obtained (Stevenson 1955).

LIGHT SOURCE AND BALANCE CIRCUIT

FOR LIFETIME MEASUREMENTS
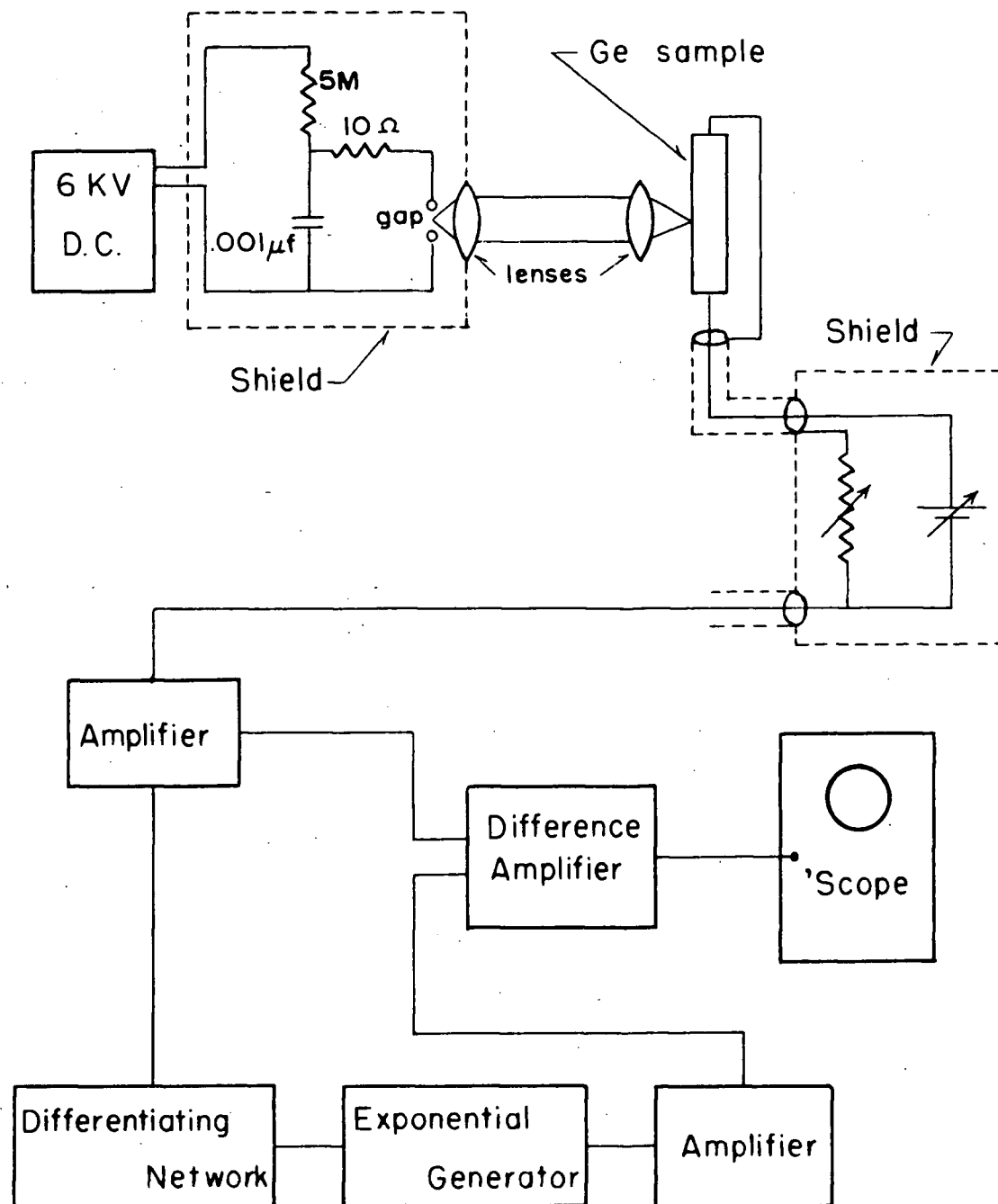
From condition (iii) the photo-conductive decay
method of lifetime measurement requires a light source
which can be switched off in a time short compared with
carrier lifetime. Since lifetimes may be as short as a
few microseconds, the light source should go from full to
zero intensity in 0.5μ sec. or less. A spark gap is the
most convenient light source capable of meeting this
requirement. Such a light source was obtained by charging
an 0.001μF condenser through a high resistance and discharg-
ing it across a gap using the circuit shown in Figure 13.
By adjusting gap width and placing a small resistance in
series with it, the light pulse duration measured with a
photo multiplier and fast oscilloscope was reduced to 0.1μ
sec. The gap consisted of an auto spark plug with approxi-
mately one millimeter between the electrodes and was operated
in air. The condenser, charging resistor, and gap were
enclosed in a metal container to reduce electrical inter-
ference and the spark was focussed on the filament using
a two lens system (see Figure 13).

Decay constants of the photo conductive pulses
were measured using a null balance method. This method
required generation of exponentially decaying pulses with
adjustable and accurately known time constants. The
generated pulses were balanced against the photo conductive
decay pulses using an oscilloscope with an input difference
amplifier. When the amplitudes of the two pulses were
equal, the decay constant of the generated pulse was adjusted

to give a zero signal.

An attempt was made to generate the desired pulses by reflecting part of the light from the spark gap to a photo multiplier whose load resistance was shunted by a variable capacitor. For this system to be satisfactory it was necessary that a given number of photons should always produce the same excess carrier density, and that a constant fraction of each light pulse be incident at the photo multiplier. Because of variation of spark path across the gap, neither of these requirements was closely attainable and this method of pulse generation was abandoned.

The technique finally developed involved generation of standard decay pulses directly from the photo conductive pulses (see Figure 13). The photo conductive pulses are amplified and fed to a 1μ sec. RC differentiating network and the resulting spikes are applied to the grid of a triode biassed to cutoff. The cathode resistor was made much larger than the tube transconductance and was paralleled by a variable capacitor. As the spike was applied to the grid the condenser was charged. Approximately a microsecond later, the tube had returned to the cutoff condition, and the capacitor discharged through the cathode resistor supplying the necessary pulse of adjustable decay time. To ensure that the generated pulse heights were proportional to the photo conductive pulse heights, it was necessary for the spike amplitude to be large compared with the difference between applied bias and cutoff bias.

The lower limit of pulse time constant measureable with this system was approximately 3μ sec. Shorter time constants were estimated directly from the photo conductive pulse displayed on the oscilloscope.

The performance of the circuit was tested by measuring an accurately known time constant of an exponentially decaying voltage pulse. The null point was sharp enough to allow a balance to within one part in four hundred of the variable capacitance, i.e., of time constant. This figure however, represents operation under optimum conditions; the pulses were of constant amplitude, exactly exponential, and free from noise. The photo conductive pulses did not have a uniform amplitude, and in most cases had an unavoidable noise background. In addition to this any pulses with amplitudes smaller than the difference between the triode applied and cutoff bias appeared without a corresponding balancing pulse, and tended to make the balance point less well defined. With these practical difficulties, the uncertainty in balance was within five per cent.
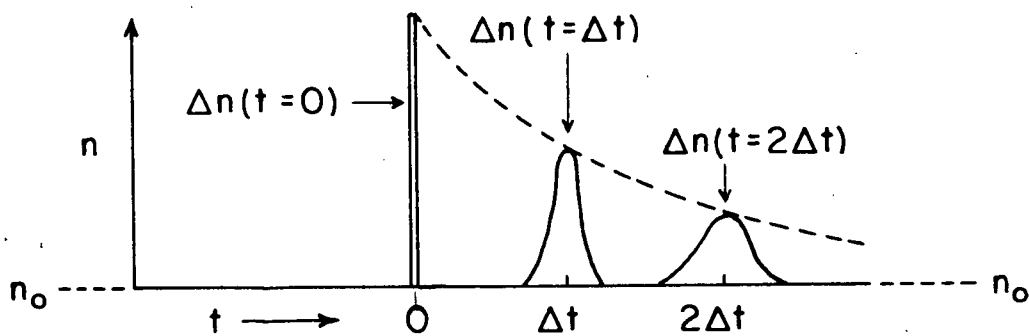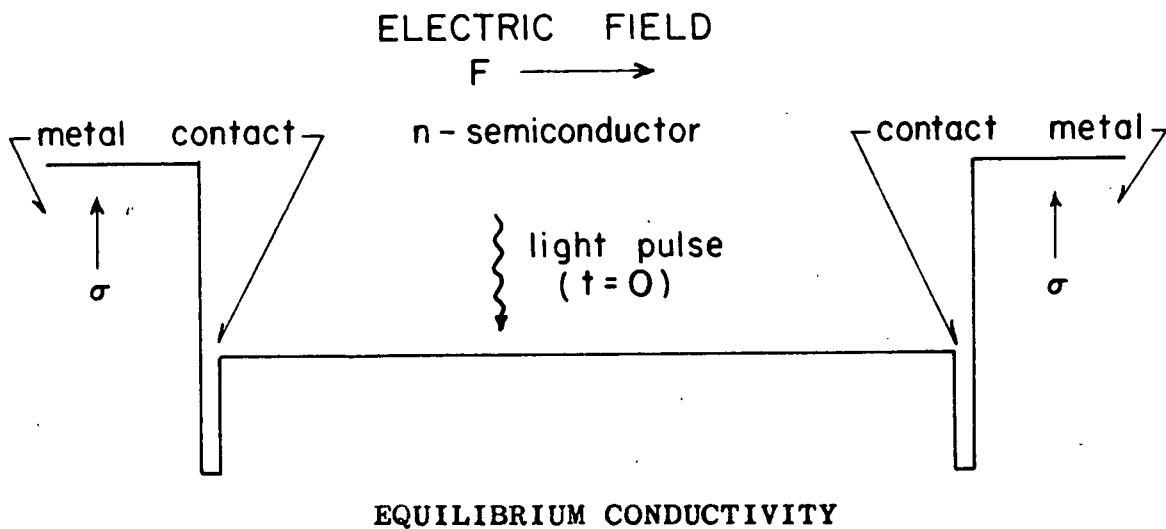
3.7 Photo-Conductive Effects

In the lifetime measurements described in section
3.6, the field applied to the filament is kept small enough
that carrier motion is predominantly diffusional

$$F < \frac{kT}{qL_a}$$

When the field is increased beyond this value, the packet of
carriers photo-generated by the spark image moves along the
filament decaying as it goes, and with a field larger than $\frac{d}{\mu_a \tau}$
carriers will be swept out of the filament before decaying
(see section 3.6). If sweep-out fields are applied to the
filament with the circuit shown in Figure 13, one expects
the observed wave-form across the resistor in series with
the filament to be a truncated exponential. The expected
wave-form was observed with the 3 ohm-cm p-type filaments
only. With filaments of the other materials the wave-form
was exponential immediately after the light impulse but
was followed by a subsequent increase in pulse height which
fell rapidly to zero (Figure 14).

With a constant field in the filament, the time
between the original spark impulse and the peak of the "after-
pulse" was proportional to the distance of the spark image
from the contact towards which the carrier packet was moving,
and approached zero as the spark image approached the
contact. With the spark image at a fixed position on the
filament, the time between the spark impulse and the after-
pulse peak was inversely proportional to the sweeping field.

PHOTO CONDUCTIVE AFTER-PULSE AT A METAL–SEMICONDUCTOR CONTACT

ELECTRIC   FIELD

F ⟶

metal   contact   n – semiconductor   contact   metal

σ light pulse
                               (t = 0) σ

EQUILIBRIUM CONDUCTIVITY

$\Delta n(t=0) \rightarrow$ $\Delta n(t=\Delta t)$

n $\Delta n(t=2\Delta t)$

n_o ----   ---- n_o

t ⟶   O Δt $2\Delta t$

ADDED CARRIER DISTRIBUTION

V (t = 0) —

Volts
across
filament

V_{dark} —

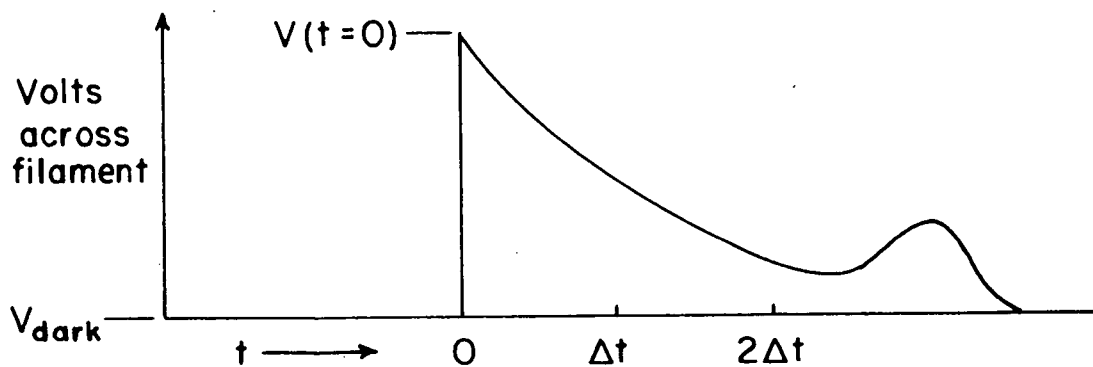t ⟶   O Δt $2\Delta t$

PHOTO CONDUCTIVE PULSE

In both cases it was necessary for the field to be large
enough to produce sweep-out. These observations indicate
that the after-pulse is associated with a contact effect.

A given density of excess carriers produces a
larger resistivity decrease in a low conductivity region
than in a high conductivity region, and this fact is used
to explain the pulse wave-forms. A pulse of light produces
a packet of photo-generated carriers in the filament which
drifts towards a contact decaying and spreading as it goes
(Figure 14). The local conductivity increase due to the
carrier packet causes a decrease of filament resistance. As
the packet decays the filament resistance returns to its
unilluminated value. However, if the crystal is inhomo-
geneous, the carriers may move into a region of lower
conductivity, resulting in a lowering of the filament resis-
tance even though the total excess carrier density is
decreasing through recombination. In our case the region
of lower conductivity is the metal-semiconductor contact (see
section 3.2) and as the carrier packet moves out of the
filament, the photo conductive after-pulse is observed. This
effect was not present in the 3 ohm-cm p-type filaments, and
this confirms the ohmic quality of contacts to this material.

CHAPTER IV - MEASUREMENTS OF BULK PHOTO E.M.F.

4.1 Linearity of the Photo e.m.f. with Weak Illumination Intensity

Most of the bulk photo e.m.f. measurements were made using filaments from the 40 ohm-cm n material and the graded material (see section 3.3). In the 40 ohm-cm material the resistivity fluctuates about a mean value throughout the length of the ingot while in the graded material the resistivity increases monotonically along the ingot. Photo e.m.f. scans of the 3 ohm-cm p and 10 ohm-cm n filaments showed bulk e.m.f.'s of a fraction of a millivolt, and although these were useful in assessing the homogeneity of the ingots, the voltages were not large enough for detailed investigation of photo e.m.f. behaviour.

In measurements of the bulk photo e.m.f., the incident light is considered "weak" if the photo-generated carrier concentration is small compared with the equilibrium majority carrier concentration. When excess carrier density is comparable with the equilibrium concentration saturation e.m.f. effects are observed (see section 2.3). Thus for our purposes illumination intensity refers to the ratio of photo generated to equilibrium carrier densities and not to photons incident per unit area per second. For example, photo generated carrier density is dependent on the filament effective lifetime (see Appendix V) and a given illumination

which approaches saturation intensity when incident on an etched surface may be weak when the surface is sandblasted. Also, the equilibrium carrier density in the intrinsic range increases rapidly with temperature and an illumination which has saturation intensity at room temperature will be weak at some higher temperature.

The light incident on the filament was varied using a stepped wedge with equal density increments per step. Optical density is defined as

$$density = \log_{10} \frac{I_i}{I_t}$$

where I_i is the incident intensity and I_t the transmitted intensity. When a collimated beam of light is incident on the wedge the total transmitted intensity consists of an attenuated beam plus forward scattered light. The diffuse density is defined with I_t equal to the total transmitted intensity and the specular density is defined with I_t equal to the intensity of the transmitted beam. The manufacturer's data for the wedge specified optical neutrality for wavelength from 0.4 to 1.0 microns and included a calibration in diffuse densities. In our experiment set-up, the transmitted beam was focussed on the filament and thus it was necessary to recalibrate the wedge for specular density. A germanium photo diode was used to make this calibration, first, because the short circuit photo current was known to be directly proportional to the incident light intensity (Cummerow 1954) and second, because its spectral sensitivity was identical with that of our filaments thus giving a

FIGURE 15

DEPENDENCE OF BULK PHOTO E.M.F.

ON ILLUMINATION INTENSITY
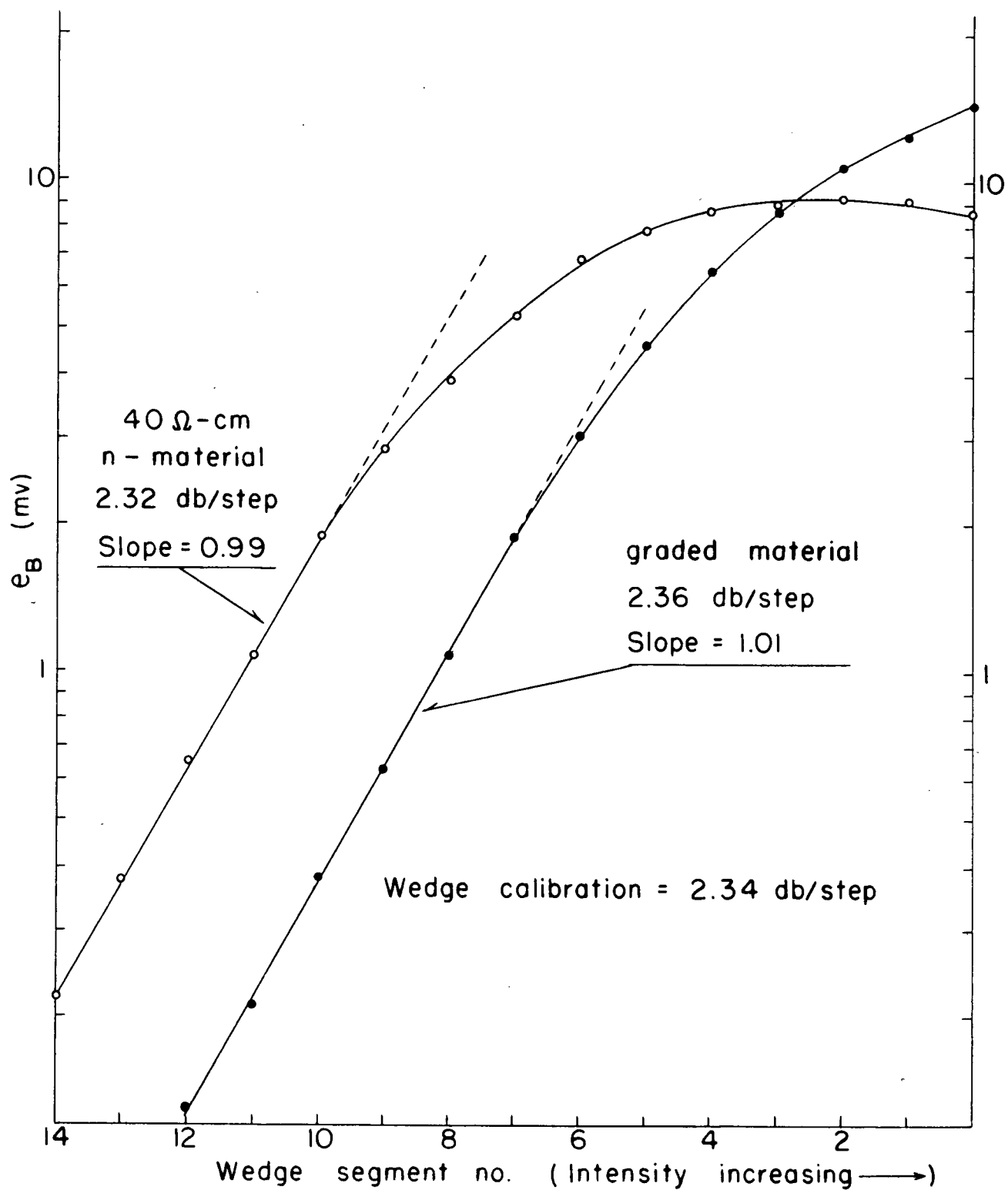
calibration which automatically took account of any departure
of the wedge from optical neutrality at wavelengths greater
than 1 micron. Using the photo diode the measured wedge
specular density was 0.234 per step, or 2.34 db per step.

The theory of the bulk photo e.m.f. predicts a
linear dependence of photo voltage on weak illumination
intensity (see section 2.3) and this was verified using the
calibrated wedge. Log photo voltage was plotted against
wedge step, and from the wedge calibration a linear relation
between voltage and illumination corresponded to a straight
line of 2.34 db per step, i.e., slope of one in log voltage
versus log illumination intensity. Observations were made
with both the 40 ohm-cm n material and the graded material
at various e.m.f. peaks in the filaments. In all cases the
slopes were between 0.94 and 1.01. Typical plots are shown
in Figure 15. These results verified the linearity of photo
e.m.f. with weak illumination intensity.

FIGURE 16

COMPARISON OF LOCAL RESISTIVITY AND BULK

PHOTO E.M.F.
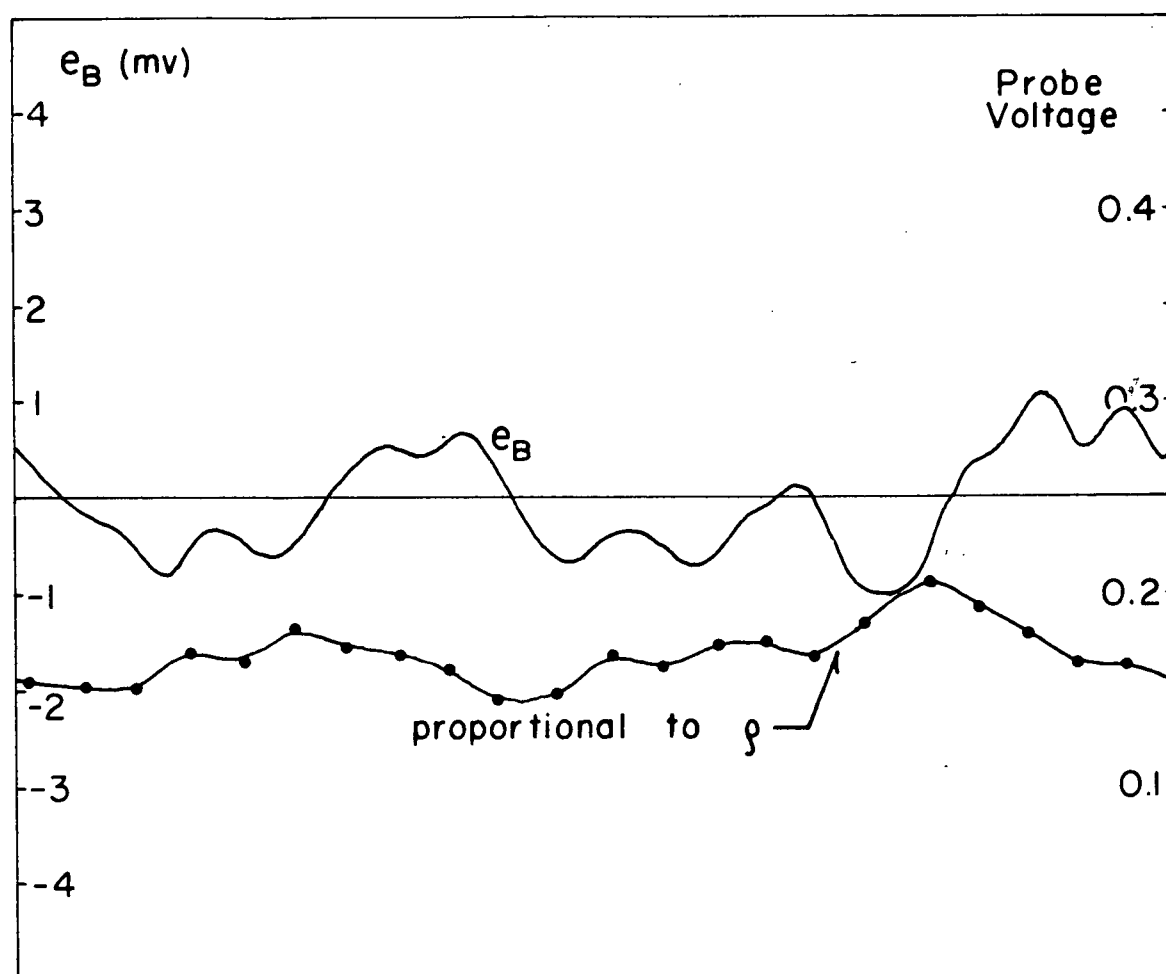
4.2 Dependence of Bulk Photo E.M.F. on Impurity Density Gradient

The bulk photo e.m.f. arises from an impurity gradient in the semiconductor and the final form of the e.m.f. expression involves the equilibrium carrier densities at the edges of illumination for both weak and saturation intensities (see section 2.3). Except in the near intrinsic case the equilibrium carrier densities may be identified with the equilibrium conductivities (see section 2.6), and in extrinsic materials the photo e.m.f. with a given illumination should have a maximum value where the impurity density gradient, i.e., conductivity gradient, has a maximum. Thus for an n-type specimen with weak illumination intensity we may write (see section 2.6)

$$ e_B = \frac{2\,kT}{b\,q} \Delta n_L \left[\frac{1}{n_{ob'}} - \frac{1}{n_{oa'}} \right] = \frac{2}{b+1} \frac{kT}{q} \Delta \sigma_L \left(\rho_{ob'} - \rho_{oa'} \right) $$

The proportionality of bulk photo e.m.f. to the differences between equilibrium resistivities at the illumination edges was experimentally checked by comparing a probe measurement of local resistivity with a photo e.m.f. pattern obtained over the same length of filament. A constant current was passed through a germanium filament and two metal probes with a fixed spacing of approximately 0.7 millimeters were moved along it. The voltage between the probes was proportional to the local resistivity, and the positional variation of this voltage is shown with the corresponding photo e.m.f. pattern in Figure 16. Points in the plot where the photo e.m.f. has a maximum or minimum correspond to

points where the resistivity gradient has a maximum or minimum, and the curves suggest that the photo e.m.f. is proportional to the local resistivity gradient as predicted by the theory. Shortly after these observations were made the proportionality of bulk photo e.m.f. to resistivity gradient was adequately confirmed by Frank (1956) and further investigation of this point was unnecessary.

The photo e.m.f. gives a measure of impurity gradient and is thus better suited for investigation of crystal inhomogeneities than probe measurements of resistivity. This is especially true in near intrinsic material where conductivity has a minimum (see section 2.6). Figure 16 illustrates the advantage of light probe measurement of impurity gradients; the fine structure in the photo e.m.f. pattern may be identified with resistivity gradients which were not detectable by the probe measurements.

4.3 Measurements of the Ratio of Bulk Photo e.m.f. to Photo Resistance

From the analysis of section 2.6 the ratio of bulk photo voltage to photo resistance should be constant at weak illumination. With a uniform density of photo-generated carriers, the ratio is directly related to the impurity density gradient, i.e.

$$\frac{e_B}{\Delta R} = - \frac{2A}{b+1} \frac{kT}{q} \frac{d\sigma_o}{dx}$$

To verify this expression experimentally, an accurate probe measurement of local conductivity, and uniform generation of carriers in the bulk of the filament are necessary. Although a non-uniform photo-generation rate corresponds to an effective crossectional area less than A (section 2.6), the ratio should remain constant at weak illumination even under this condition.

For measurement of the ratio of bulk photo e.m.f. at weak illumination, the light spot was focussed on a position in a filament exhibiting a large e.m.f. peak. The stepped wedge was used to decrease the light intensity by known increments, and the photo e.m.f. was measured by a potentiometer. The illuminated and dark resistance measured on a wheatstone bridge gave the photo resistance. The added carrier distribution must be the same in the e.m.f. and resistance measurements, and for this reason an a.c. bridge source is preferable. The bridge balance point was deter- mined using a high gain oscilloscope with an input difference

DEPENDENCE OF PHOTO RESISTANCE AND BULK PHOTO E.M.F.

ON ILLUMINATION INTENSITY
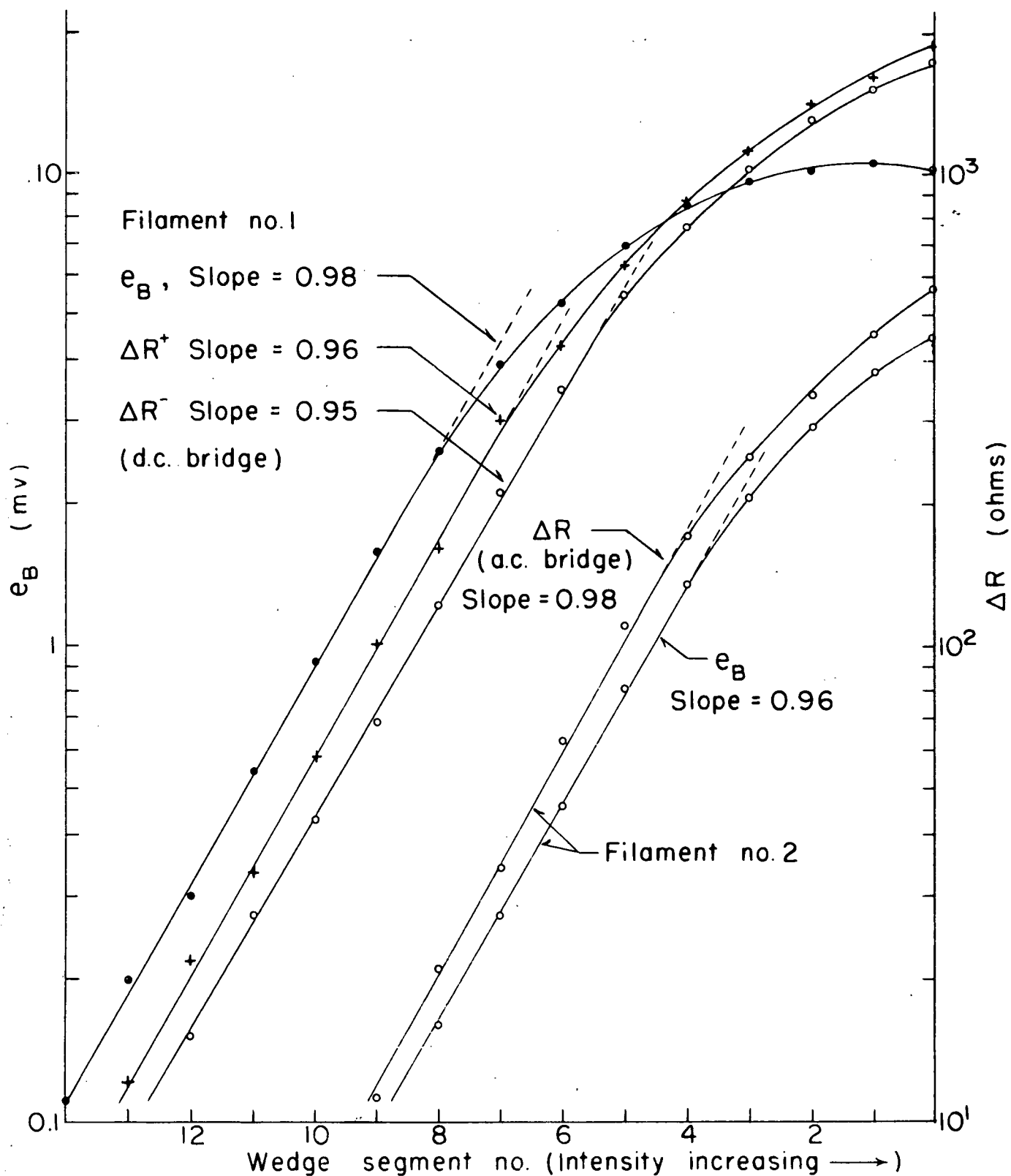
amplifier. Plots of log photo resistance and log photo voltage were parallel with a slope of approximately one (Figure 17). These observations show that the ratio of photo e.m.f. to photo resistance was constant at weak illumination as predicted by theory. However, since the photo-generated carrier density was not uniform throughout the filament crossectional area, the results could not be used for a quantitative verification of the expression for the ratio of photo voltage to photo resistance.

Photo resistance measurements were also made using a d.c. bridge source. In this case the field applied to the filament must be kept small enough that carrier motion is predominantly diffusional, i.e.,

$$F < \frac{kT}{qL_a}$$

The maximum allowable field from this condition was small enough that the photo e.m.f. substantially affected the bridge balance. This difficulty was removed by bucking out the photo voltage with an equal and opposite voltage applied across a known resistance in series with the filament. With this method, the photo resistance was found to be dependent on direction of current flow, and plots of log photo resistance against log light intensity were parallel to each other and to the log photo voltage plot (Figure 17).

The change of photo resistance with current direction was explained by the dependence of dark and illuminated resistance on current density. The dark resistance of the

filament used for the d.c. bridge measurements showed
considerable asymmetry with current densities in opposite
directions. With light incident on the photo e.m.f. peak,
this asymmetry decreased with light intensity and at strong
illumination the filament resistance was not affected
by the direction of current up to the maximum allowable
from the diffusional condition. Thus the observed dependence
of photo-resistance on current direction originated in the
asymmetry of the dark resistance with current density. When
the filament was illuminated at a point where the photo
voltage was zero, the illuminated resistance showed a depen-
dence on current density similar to the dark resistance.

The characteristics of the dark and illuminated
resistances corresponded to a weakly rectifying junction at
the point of illumination. This region exhibited a large
peak photo voltage, i.e., had a large local impurity gradient,
and the asymmetry in the dark resistance as a function of
current density corresponded to the direction of rectification
implied by the polarity of the photo e.m.f. The voltage
drop across the weak junction was sufficient to perturb the
added carrier distribution from its open circuit value even
though the total field applied to the filament conformed to
the diffusional condition. This could account for the change
in photo resistance with current direction.

At saturation illumination intensity, the electro-
static potential step associated with the impurity gradient
was flattened out, and the cause of rectifying behaviour
removed. As a result the illuminated resistance of the

filament showed less non-ohmic behaviour than the dark
resistance. These observations showed that the electrical
contacts to some of the 40 ohm-cm n filaments were better
than was indicated by the methods of section 3.2 in the
sense that a part of the observed non-ohmic behaviour
originated in the bulk of the filaments.

At the higher light intensities the ratio of photo
e.m.f. to photo resistance was measured using a method
described by Tauc (1957). A constant current was passed
through the filament and the light beam chopped using a
rotating slotted disc. The light pulse incident on the
filament produced a photo resistance pulse which appeared
at the filament terminals as a voltage pulse equal to the
product of current and photo resistance. When the light
was incident on a region of impurity density gradient, a
photo voltage pulse also appeared at the terminals. The
resultant voltage across the filament was displayed on a
high gain oscilloscope, and the direction and magnitude
of the current was adjusted to reduce the observed pulse
to zero. At this point

$$\frac{e_\beta}{\Delta R} = i_f$$

where i_f is the current through the filament. With photo
voltages of the order of a millivolt the oscilloscope gain
was not sufficient to allow an accurate pulse balance,
however, photo voltages of this magnitude are ordinarily
in the linear range (Figure 17) where the ratio of photo

voltage to photo resistance is known to be constant. The accuracy of the compensation method described above improves with increasing photo voltage and was used chiefly to investigate the behaviour of the ratio in the saturation range of illumination intensities.

FIGURE 18
SATURATION EFFECTS

(a) STRONG ILLUMINATION DEPENDENCE OF LIGHT PROBE DIMENSIONS
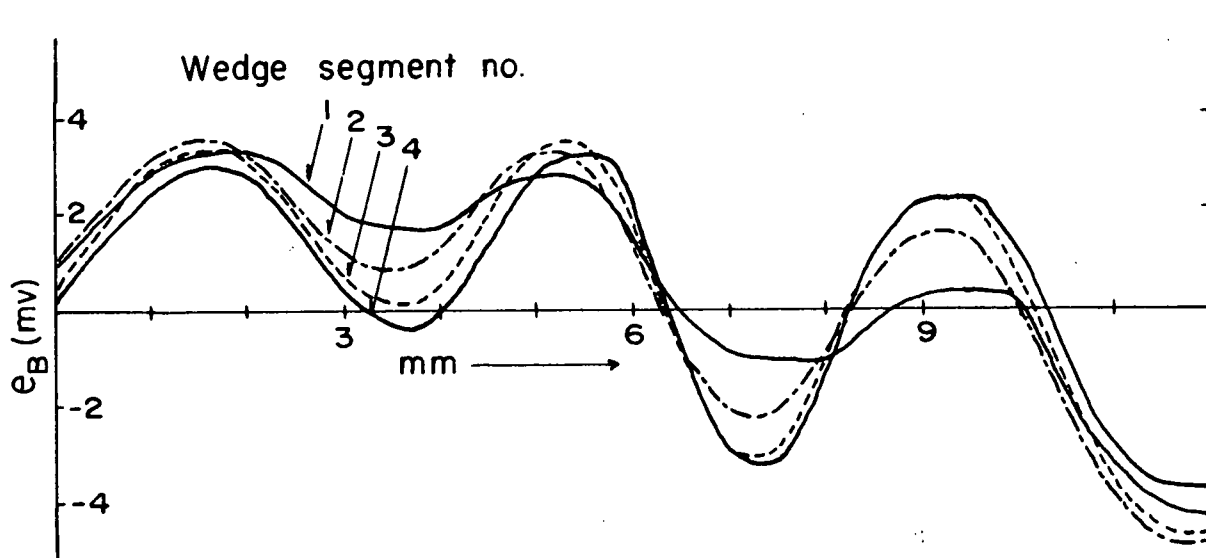
(b) STRONG ILLUMINATION CHARACTERISTICS OF PHOTO VOLTAGE AND
PHOTO RESISTANCE

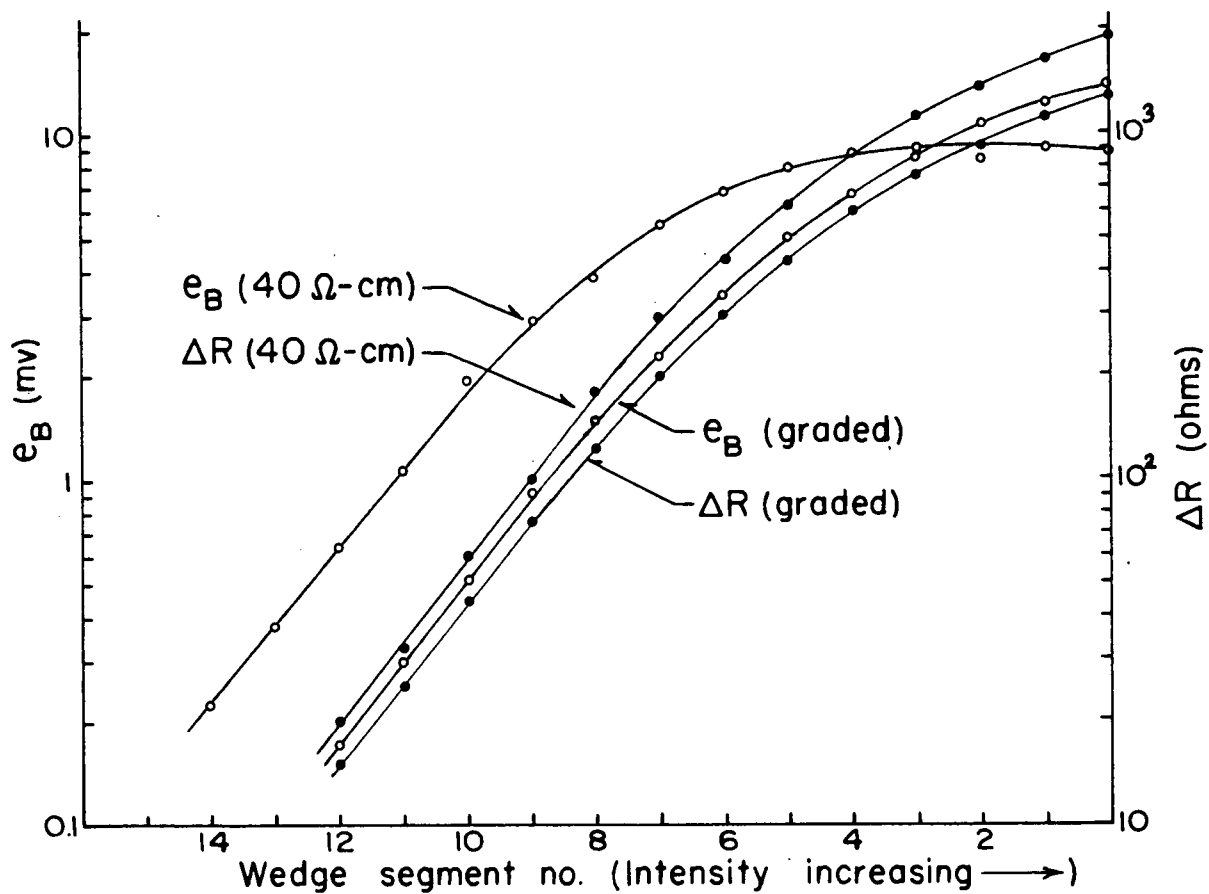## 4.4 <u>Saturation Effects</u>

When the illumination intensity is sufficient to produce saturation e.m.f. in the volume under the illuminated area, a further increase in intensity affects the photo e.m.f. only through carriers which have diffused far enough to arrive in an unsaturated region. These unsaturated components will always be present in the observed e.m.f. unless the impurity density gradient occurs only in the region where light is incident. Since this is not normally the case, the observed "saturation" e.m.f. will increase or decrease with light intensity depending on the impurity distribution in the immediate neighbourhood of the light spot (see section 2.6). If the light spot is considered a sampling probe, an increase of illumination intensity into the saturation range may be thought of as increasing the probe dimensions beyond $2(a + L_p)$ (see section 2.3).

In the 40 ohm-cm n material, the impurity density fluctuates about a mean over the length of a given filament (Figure 16). In this material the unsaturated components will generally have a polarity opposite to the saturated component, and the photo e.m.f. will decrease as the illumination intensity is increased into the saturation range. This is illustrated in Figure 18(a) which consists of records of successive scanning of a heavily etched 40 ohm-cm filament with illumination intensity decreasing in the saturation range. The corresponding decrease in probe dimensions permits a better resolution of the e.m.f. peak

and a consequent higher e.m.f. at lower illumination intensities.

In the graded material the impurity density increases monotonically along the filament and all e.m.f. components are of the same polarity. In this case the photo e.m.f. continues to increase up to the maximum illumination intensity. The dependence of photo e.m.f. and photo resistance on light intensity is shown in Figure 18(b). In both materials the photo resistance behaviour is the same, and because of the impurity distribution in the graded material the ratio of photo voltage to photo resistance is constant up to the maximum illumination intensity. This is discussed in section 2.6.

4.5 Temperature Dependence of the Bulk Photo E.M.F.

The temperature dependence of the bulk photo e.m.f. can be calculated from the results of section 2.3. For weak illumination in extrinsic material

$$e_B = \frac{2kT}{qb} \Delta n_L \left[\frac{1}{n_{ob'}} - \frac{1}{n_{oa'}} \right] \qquad \text{in n-type}$$

and

$$e_B = -\frac{2bkT}{q} \Delta n_L \left[\frac{1}{p_{ob'}} - \frac{1}{p_{oa'}} \right] \qquad \text{in p-type}$$

The impurity centers may be assumed totally ionized in germanium at temperatures greater than 50°K and thus the equilibrium concentrations are independent of temperature. The temperature dependence of b, the ratio of mobilities of electrons and holes is calculated from published mobility data (Morin 1954)

$$b = \frac{4.9 \times 10^7 \ T^{-1.66}}{1.05 \times 10^9 \ T^{-2.33}} = 4.65 \times 10^{-2} \ T^{0.66}$$

The added carrier concentration Δn_L is dependent on life-time, and if the carrier lifetime is temperature dependent this will influence the temperature dependence of the bulk photo e.m.f. Where lifetimes are constant in the extrinsic material

$$e_B \propto \frac{T}{b} \propto T^{0.33} \qquad \text{in n-type}$$

$$e_B \propto bT \propto T^{1.66} \qquad \text{in p-type}$$

In near intrinsic material (section 2.5)

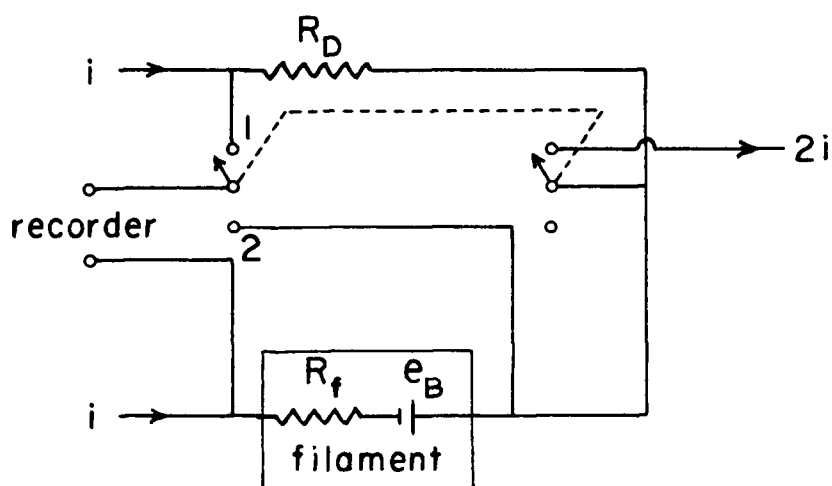$$e_B = -\frac{2b}{(b+1)^2} \frac{kT}{q} \Delta n_L \frac{(N_D - N_A)_{b'} - (N_D - N_A)_{a'}}{n_i^2}$$

In this expression the temperature dependence of the factor involving the mobility ratio may be neglected, and where Δn_L is temperature independent
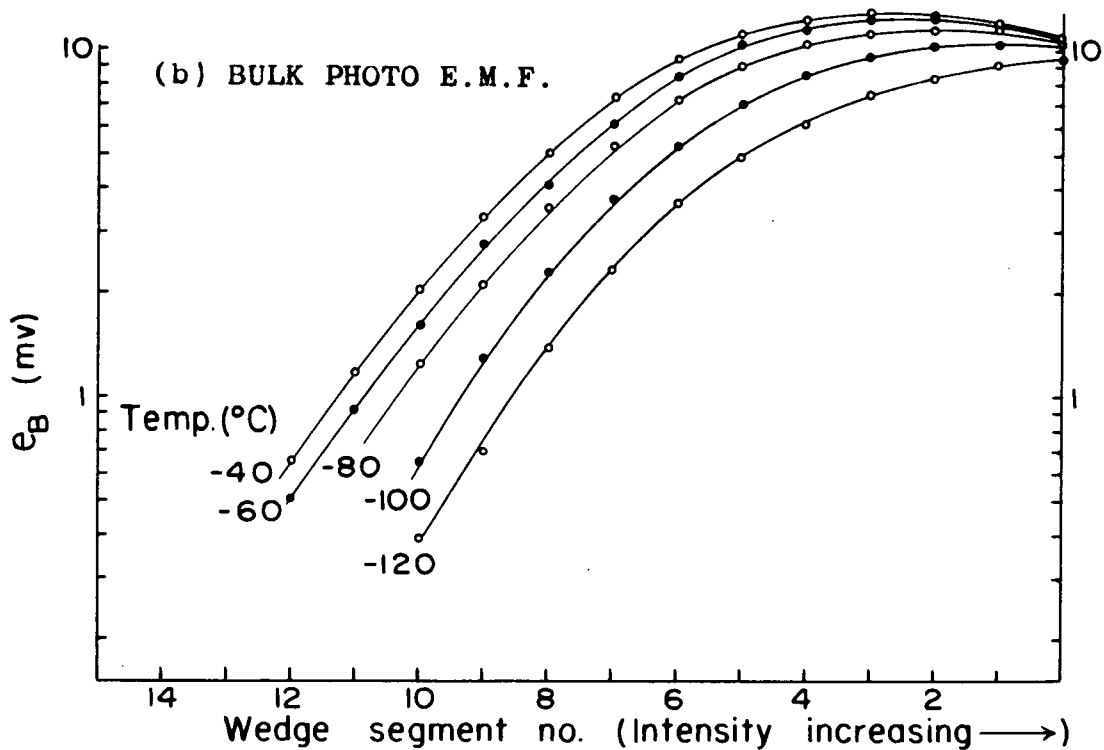
$$\frac{e_B}{T} \propto \frac{1}{n_i^2}$$

Observations of the bulk photo e.m.f. temperature dependence were made over a temperature range of -120°C to 100°C. For measurements at low temperatures the filament was placed in a dewar flask with an aperture in the silvering, and the light was focussed on a position exhibiting a large photo e.m.f. peak. The temperature was lowered by pumping liquid nitrogen through a coil of copper tubing inside the dewar and temperature measurements were made by means of a thermocouple connected to one contact of the filament. To minimize temperature differences between the contacts, the filament was mounted horizontally. In the first measurements the dewar was filled with petroleum ether to provide thermal inertia and stabilize the temperature in the region of the specimen. This was unsatisfactory at the lower temperatures as the petroleum ether became increasingly cloudy below -30°C. and froze at approximately -80°C. Since no other suitable coolant was available, the petroleum ether was removed and the filament temperature was lowered by cooling the surrounding air in the flask.

When a sufficiently low temperature was reached, the pump was shut off and measurements of the photo e.m.f as a function of illumination intensity were made at 10° intervals as the filament warmed to room temperature. One disadvantage of this arrangement was the rapid rate of warming at low temperatures which made it difficult to get complete observations of the photo e.m.f. as a function of illumination intensity before the temperature had changed appreciably.

After the necessary experimental techniques for measuring the bulk photo e.m.f. at low temperatures had been developed, the filament was incorporated into a circuit which allowed concurrent measurement of both the bulk photo e.m.f. and photo resistance. Two equal constant currents were passed through the filament and a variable resistor which was made equal to the filament dark resistance.

TEMPERATURE DEPENDENCE IN THE EXTRINSIC

RANGE OF CONDUCTIVITY

(a) PHOTO RESISTANCE

ΔR (ohms)

Temp.(°C)

-40
-60
-80 -100 -120

Wedge segment no. (Intensity increasing ⟶)

(b) BULK PHOTO E.M.F.

e_B (mv)

Temp.(°C)

-40
-60 -80
-100
-120

Wedge segment no. (Intensity increasing ⟶)
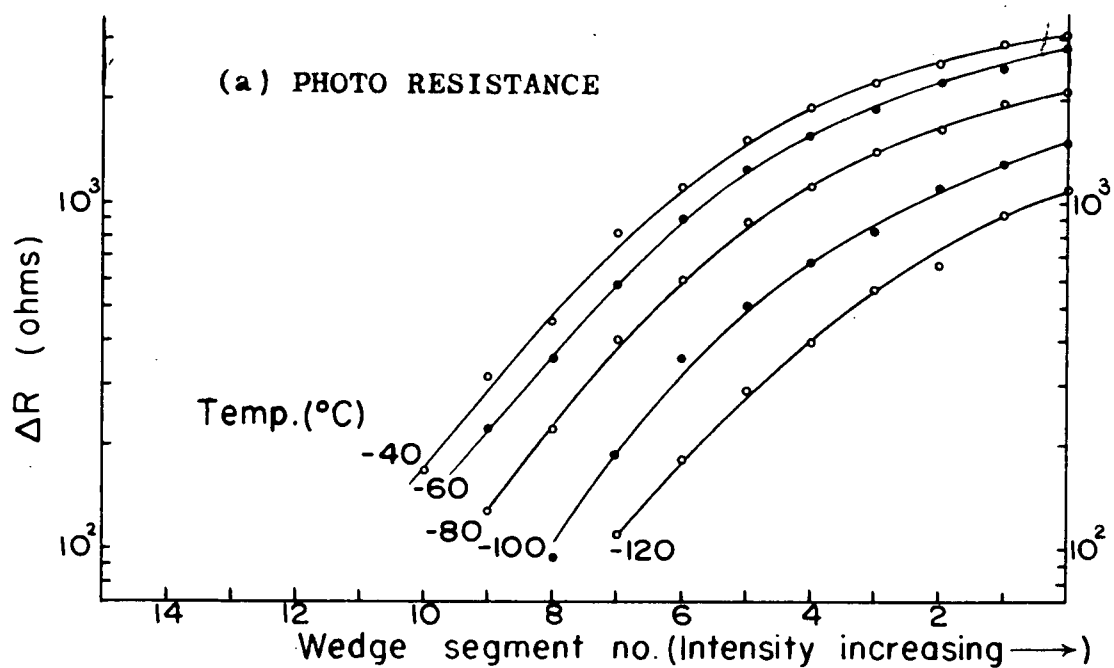
With the switch in position 1 as shown, one terminal of
each of the resistor and the filament was connected together
and the voltage between the other terminals (i) was zero
with no illumination and (ii) with filament illuminated
was equal to the bulk photo voltage plus the product of
current and photo resistance. This voltage was measured
on a recording 0-10 mv meter. With the switch in position
2, the current was shut off and the photo voltage recorded.
By subtracting the two voltages a value of the photo
resistance was obtained. This method of measuring photo
resistance is subject to considerable error at weak illumina-
tion but the accuracy improves at strong illumination where
the difference between the two voltages is greater. Since
the photo resistance is known to be directly proportional
to the photo e.m.f. at weak illumination (see section 4.3),
inaccuracy at low light intensity is not a serious
disadvantage.

At temperatures from -120°C. to -30°C. both the
photo e.m.f. and photo resistance increased with temperature
(Figure 19a and b) in a 40 ohm-cm filament. As the tempera-
ture was increased further, both quantities decreased slowly
until the temperature had reached approximately 10°C., and
then decreased more rapidly as the filament entered the
intrinsic range of conductivity. With the graded filament
the behaviour of photo e.m.f. and photo resistance was
similar to that described for the 40 ohm-cm filament.

With both materials the increase of photo e.m.f.
with temperature in the extrinsic range is too rapid to be

TEMPERATURE DEPENDENCE OF THE BULK PHOTO E.M.F.

IN THE INTRINSIC RANGE
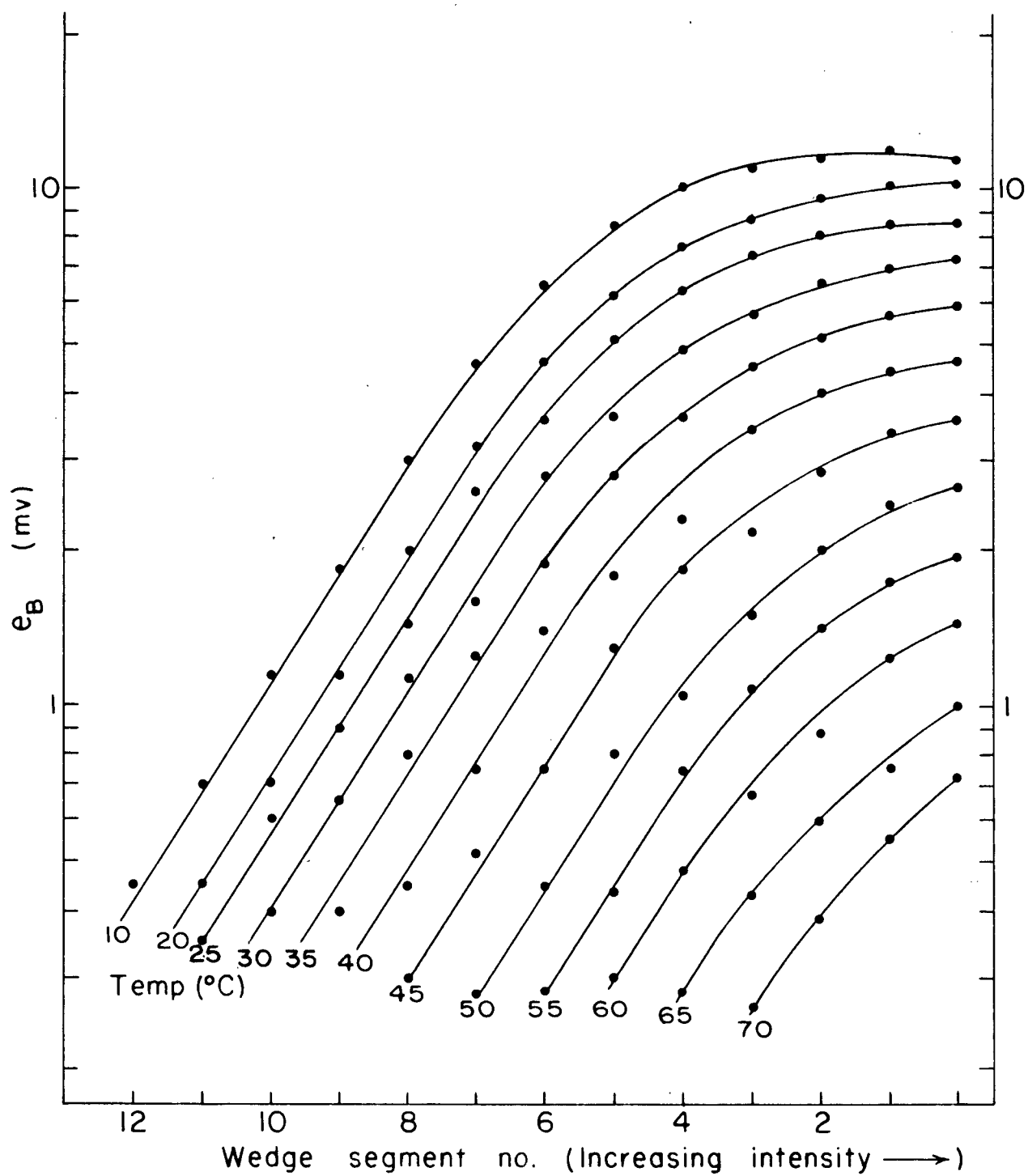
accounted for by the T/b term (see above) and is attributed
to the lifetime dependence of the Δn_L factor. This is
borne out by the photo voltage versus illumination charac-
teristics for the 40 ohm-cm material which shows a
progressive decrease of e.m.f. with light intensity at strong
illumination from $-120°$C. to $-40°$C. This corresponds to an
increase in the effective light intensity, i.e. increasing
lifetime (see sections 3.2 and 4.1).

In successive low temperature measurements, the
magnitude of the photo e.m.f. with a given light intensity
was not closely reproducible, In all cases however, the
photo e.m.f. and photo resistance were linear with weak
illumination intensity and the curves showed the other
characteristics of Figure 19. By drying the air in the dewar
flask the variation between successive sets of low temperature
measurements was reduced, but not entirely removed. Because
of this behaviour, an analysis of Δn_L through lifetime
measurements at low temperatures was not attempted.

The same methods of measurement were used to investi-
gate temperature dependence of the photo e.m.f. in the
intrinsic range. The filament was heated in air in a dewar
flask and at a sufficiently high temperature the heater was
shut off and observations of photo e.m.f. as a function of
illumination intensity were made as the filament cooled to
room temperature (Figure 20). The photo e.m.f. showed
progressively less saturation behaviour as the temperature
was increased because of the rapid increase of equilibrium
carrier concentration, and consequent decrease in the ratio

FIGURE 21

EXPERIMENTAL VERIFICATION OF THE THEORY OF THE BULK

PHOTO E.M.F. IN THE INTRINSIC RANGE
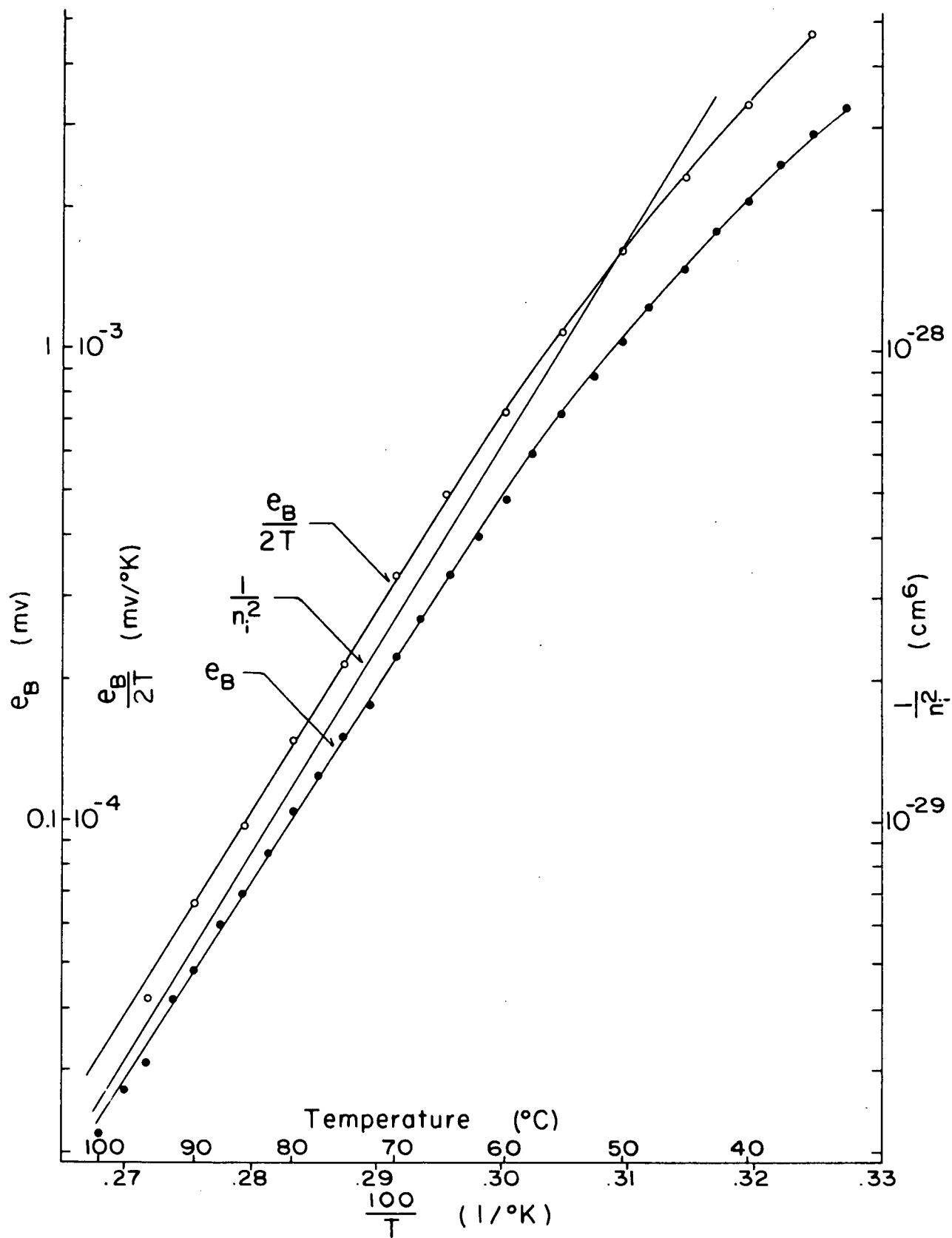
of photo-generated to equilibrium carrier densities (see section 4.1).

At temperatures above room temperature, successive sets of photo e.m.f. observations were accurately reproducible, and it was possible to obtain an experimental check on the weak illumination temperature dependence of the photo e.m.f. predicted by the theory. The measurements were made from 20°C. to 100°C. in the manner described above except that the light intensity was maintained constant and the photo voltages were measured on a potentiometer. The carrier lifetime decreased slowly with increasing temperature, showing a total change of approximately 10% over the temperature range investigated. Thus the Δn_L factor has negligible effect on the bulk photo e.m.f. temperature dependence and from the theory (see above)

$$\frac{e_B}{T} \propto \frac{1}{n_i^2}$$

The value of n_i^2 was taken from published data (Morin 1954)

$$n_i^2 = 3.1 \times 10^{32} \, T^3 \exp\left[-\frac{0.785}{kT}\right]$$

This relationship was checked by plotting log e_B and log $e_B/2T$ as a function of reciprocal temperature, and comparing the slope of the plot with log $1/n_i^2$ as a function of reciprocal temperature (Figure 21). The slope of the log $e_B/2T$ and log $1/n_i^2$ plots are equal within experimental error, and this confirms this feature of the theoretical treatment of the bulk photo e.m.f. in the intrinsic range.

A P P E N D I X   I

Imref Gradients with Large Added Carrier Concentrations

Equal added carrier densities n_a and p_a are present at the plane $x = 0$. If all carrier motion is diffusional, then

$$p(x) = p_o + p_a \exp\left[-\frac{x}{L_a}\right]$$

$$n(x) = n_o + n_a \exp\left[-\frac{x}{L_a}\right]$$

where L_a is the ambipolar diffusion length.

Then

$$\left[\phi_p(x) - \psi(x)\right] = \frac{kT}{q} \ln\left[\frac{p_o + p_a \exp\left(-\frac{x}{L_a}\right)}{n_i}\right]$$

and

$$\text{grad}\left[\phi_p(x) - \psi(x)\right] = -\frac{kT}{qL_a}\left[\frac{p_a \exp\left(-\frac{x}{L_a}\right)}{p_o + p_a \exp\left(-\frac{x}{L_a}\right)}\right]$$

In extrinsic material where carrier motion is predominantly diffusional, grad $\phi_p(x)$ will be large compared with

grad $\psi(x)$ and where $p_a \exp\left[-\frac{x}{L_a}\right] >> p_o$

then

$$\left|\text{grad } \phi_p(x)\right| = \frac{kT}{qL_a}$$

Similarly if $n_a \exp\left[-\frac{x}{L_a}\right] >> n_o$

then

$$\left|\text{grad } \phi_n(x)\right| = \frac{kT}{qL_a}$$

In extrinsic semiconductors, the added minority carrier density from injection or photo generation may be large compared with the equilibrium minority density but is usually negligible compared with the equilibrium majority carrier density. In this case the diffusion length is that of the minority carriers (Rittner 1954) and the imref gradients are approximately

$$\left| grad \; \phi_p(x) \right| = \frac{kT}{qL_p} \quad in \; n\text{-}type$$

$$\left| grad \; \phi_n(x) \right| = \frac{kT}{qL_n} \quad in \; p\text{-}type$$

where L_n and L_p are electron and hole diffusion lengths.

A P P E N D I X   II

Dependence of Electrostatic Potential on Added Carrier Concentrations

A non-homogeneous semiconductor is illuminated producing a uniform concentration of added carriers throughout the bulk under the illuminated area. The concentrations of the electrons and holes are

$$n = n_i \, \exp \frac{q}{kT} \left(\psi - \phi_n \right)$$

$$p = n_i \, \exp \frac{q}{kT} \left(\phi_p - \psi \right)$$

and the concentration gradients are

$$\frac{grad \, n}{n} = \frac{q}{kT} \, grad \left(\psi - \phi_n \right)$$

$$\frac{grad \, p}{p} = \frac{q}{kT} \, grad \left(\phi_p - \psi \right)$$

No net current flows in the open circuit condition so that

$$b \, n \, grad \, \phi_n + p \, grad \, \phi_p = 0$$

and we use this relation to substitute for grad ϕ_p in terms of grad ϕ_n .

Thus
$$\frac{p \, grad \, n}{n \, grad \, p} = \frac{grad \left(\psi - \phi_n \right)}{-\frac{bn}{p} \, grad \, \phi_n - grad \, \psi}$$

and

$$\text{grad } \psi = \frac{n \text{ grad}(p-bn)}{\text{grad}(np)} \text{ grad } \phi_n$$

Similarly $$\text{grad } \psi = \frac{p \text{ grad}(bn-p)}{b \text{ grad}(np)} \text{ grad } \phi_p$$

If the semiconductor is homogeneous, (assumption (a), section 2.3)

$$\text{grad } n_o = \text{grad } p_o = 0$$

and

$$\text{grad } n = \text{grad } p = \text{grad } \Delta n$$

where Δn is the concentration of added electrons and holes. The above equations are simplified in this case and become

$$\text{grad } \psi = \frac{(b-1) p \text{ grad } \phi_p}{b(n+p)} = \frac{-(b-1) n \text{ grad } \phi_n}{n+p}$$

In the homogeneous semiconductor the electrostatic potential gradient can also be expressed in terms of the gradient of added carrier concentration. Since $\text{grad } n = \text{grad } \Delta n$

then $$\text{grad } \phi_n = -\frac{kT}{q} \frac{\text{grad } \Delta n}{n} + \text{grad } \psi$$

which leads to

$$\text{grad } \psi = (b-1) \frac{kT}{q} \frac{\text{grad } \Delta n}{bn+p}$$

and in intrinsic material where $n = p$

$$\text{grad } \psi = \frac{(b-1)}{(b+1)} \frac{kT}{q} \frac{\text{grad } \Delta n}{n}$$

A P P E N D I X   III

Evaluation of the Integrals

$$e_B = \int_a^b grad\left(\psi - \psi_0\right) dx$$

$$= \frac{kT}{q} \int_a^b \left[\frac{(b-1)\, grad\, \Delta n}{p_0 + bn_0 + (b+1)\Delta n} - \frac{(b-1)\Delta n\, grad\, n_0}{bn_0^2 + \Delta n(b+1)n_0 + n_i^2} \right] dx$$

The first term is identified with the diffusional e.m.f., e_d. From assumption (f) section 2.3, a significant gradient of added carrier density exists only at a' and b', the edges of illumination (Figure 6), and the first term of integrand is finite only at these points. The equilibrium carrier densities are slowly varying functions of position and may be considered constant at the two points where the integrand exists. Thus we write

$$e_d = \int_a^b = \int_{a'-\epsilon}^{a'+\epsilon} + \int_{b'-\epsilon}^{b'+\epsilon}$$

where ϵ is very small and

$$e_d = \frac{kT}{q} \frac{(b-1)}{(b+1)} \ln \frac{1 + (b+1)\Delta n_L / p_{0a'} + bn_{0a'}}{1 + (b+1)\Delta n_L / p_{0b'} + bn_{0b'}}$$

The second term is identified with the inner field component of e.m.f., e_c. In this case the integrand exists only in the region where an added carrier concentration exists, i.e., between the points a' and b'. The added carrier concentration is assumed to be constant, Δn_L , between these points (Figure 6) and the variable of integration is the equilibrium carrier density. Thus the integral becomes

$$e_c = -\frac{kT}{q} \Delta n_L \int_{a'}^{b'} \frac{(b+1)\, dn_o}{b n_o^2 + \Delta n_L (b+1) n_o + n_i^2}$$

which is readily evaluated giving

$$e_c = -\frac{2kT}{q} \frac{\Delta n_L (b+1)}{\sqrt{D}} \left[\mathrm{Tan}^{-1} \frac{2 b n_o + \Delta n_L (b+1)}{\sqrt{D}} \right]_{a'}^{b'}$$

when D is positive

$$e_c = -\frac{kT}{q} \frac{\Delta n_L (b+1)}{\sqrt{-D}} \ln \frac{2 b n_o + (b+1)\Delta n_L - \sqrt{-D}}{2 b n_o + (b+1)\Delta n_L + \sqrt{-D}}$$

when D is negative

$$D = 4 n_i^2 b - (b+1)^2 \Delta n_L^2$$

These solutions are unwieldy, and it is more convenient to consider the two extremes of weak and strong illumination i.e., added carrier density Δn_L much smaller or much larger

than the equilibrium majority carrier densities.

(a) Weak Illumination

When $\Delta n_L \ll p_o + b n_o$, the diffusional component
of the e.m.f. is approximately

$$e_d = \frac{kT}{q} (b+1) \Delta n_L \left[\frac{1}{p_{oa'} + b n_{oa'}} - \frac{1}{p_{ob'} + b n_{ob'}} \right]$$

In the inner field component we assume

$$(b+1)^2 \Delta n_L^2 \ll 4 n_i^2 b$$

Then since $\tan \theta \doteq \theta$ if θ is small

$$e_c = - \frac{kT}{q} (b+1) \frac{\Delta n_L (n_{ob'} - n_{oa'})}{n_i^2 + b n_{ob'} n_{oa'}}$$

$$= \frac{kT}{q} (b+1) \Delta n_L \left[\frac{-1}{p_{ob'} + b n_{oa'}} + \frac{1}{p_{oa'} + b n_{ob'}} \right] .$$

and

$$e_B = e_d + e_c = \frac{2 kT}{q b} \Delta n_L \left[\frac{1}{n_{ob'}} - \frac{1}{n_{oa'}} \right]$$

in n-type material $(b n_o \gg p_o)$

Or

$$e_B = e_d + e_c = - \frac{2 b kT}{q} \Delta n_L \left[\frac{1}{p_{ob'}} - \frac{1}{p_{oa'}} \right]$$

in p-type material $\left(p_o \gg b n_o \right)$

(b) Strong Illumination

When $\Delta n_L \gg p_o + b n_o$, the diffusional e.m.f. component becomes approximately

$$e_d = \frac{kT}{q} \frac{(b-1)}{(b+1)} \ln \frac{p_{ob'} + b n_{ob'}}{p_{oa'} + b n_{oa'}}$$

In the inner field component of e.m.f. the log form of the integral solution is used, and assuming $(b+1)^2 \Delta n_L^2 \gg 4 n_L^2 b$

$$e_c = -\frac{kT}{q} \ln \frac{n_{ob'}}{n_{oa'}}$$

If the substitution in the original integral expression is made in terms of p_o, then

$$e_c = \frac{kT}{q} \ln \frac{p_{ob'}}{p_{oa'}}$$

The complete expression for strong illumination or saturation e.m.f. is then

$$e_B = e_d + e_c = -\frac{2}{b+1} \frac{kT}{q} \ln \frac{n_{ob'}}{n_{oa'}}$$

in n-type material $(b n_o \gg p_o)$

or $\qquad e_B = e_d + e_c = \frac{2b}{b+1} \ln \frac{p_{ob'}}{p_{oa'}}$

in p-type material $(p_o \gg b n_o)$

A P P E N D I X   IV

Imref Derivation of the Photo e.m.f.

Using the gradients of the carrier concentrations and relating the imref gradients through the open circuit current condition

$$b\, nq\, \text{grad}\, \phi_n + p\, q\, \text{grad}\, \phi_p = 0$$

we may write

$$-\text{grad}\, \phi_n = \frac{kT}{q}\, \frac{1}{n}\, \frac{\text{grad}(np)}{bn+p}$$

and

$$\text{grad}\, \phi_p = \frac{bkT}{q}\, \frac{1}{p}\, \frac{\text{grad}(np)}{bn+p}$$

This is expanded to a more suitable form using assumption (a) section 2.3, $\Delta n = \Delta p$ and $\text{grad}\,\Delta n = \text{grad}\,\Delta p$. The expression then contains terms which may be identified with the diffusional and inner field components of the e.m.f. The integration will be carried through using the electron imref.

$$e_B = \int_a^b \text{grad}\, \phi_n\, dx$$

$$= -\frac{kT}{q}\int_a^b \frac{(n+p)\,\text{grad}\,\Delta n}{n(bn+p)}\, dx - \frac{kT}{q}\int_a^b \frac{\Delta n\,\text{grad}\,(n_o + p_o)}{n(bn+p)}\, dx$$

The first term is written

$$e_d = -\frac{kT}{q} \int_a^b \frac{(n_o + p_o + 2\Delta n)\, d\Delta n}{(n_o + \Delta n)\left[p_o + bn_o + (b+1)\Delta n\right]}$$

and expanded by partial fractions to

$$e_d = -\frac{kT}{q} \int_a^b \frac{d\Delta n}{n_o + \Delta n} + \frac{kT}{q}(b-1) \int_a^b \frac{d\Delta n}{p_o + bn_o + (b+1)\Delta n}$$

These integrals are evaluated using the methods outlined in Appendix III, giving

$$e_d = -\frac{kT}{q} \ln\left[\frac{n_{oa'} + \Delta n_L}{n_{oa'}} \frac{n_{ob'}}{n_{ob'} + \Delta n_L}\right]$$

$$+ \frac{kT}{q} \frac{(b-1)}{(b+1)} \ln \frac{1 + (b+1)\Delta n_L / p_{oa'} + bn_{oa'}}{1 + (b+1)\Delta n_L / p_{ob'} + bn_{ob'}}$$

Using the relation $\operatorname{grad} p_o = -n_i^2 / n_o^2 \operatorname{grad} n_o$ the second term is written

$$e_c = -\frac{kT}{q} \int_a^b \frac{\Delta n (n_o^2 - n_i^2)\, dn_o}{n_o(n_o + \Delta n)\left[bn_o + \Delta n(b+1)n_o + n_i^2\right]}$$

and expanded to

$$e_c = \frac{kT}{q} \int_{a'}^{b'} \frac{dn_o}{n_o} - \frac{kT}{q} \int_{a'}^{b'} \frac{dn_o}{n_o + \Delta n_L} - \frac{kT}{q} \Delta n_L (b+1) \int_{a'}^{b'} \frac{dn_o}{bn_o^2 + \Delta n_L(b+1)n_o + n_i^2}$$

These are evaluated giving

$$e_c = \frac{kT}{q} \ln \left[\frac{n_{ob'}}{n_{oa'}} \frac{n_{oa'} + \Delta n_L}{n_{ob'} + \Delta n_L} \right]$$

$$- \frac{2kT}{q} \frac{\Delta n_L (b+1)}{\sqrt{D}} \left[Tan^{-1} \frac{2bn_o + \Delta n_L (b+1)}{\sqrt{D}} \right]_{a'}^{b'}$$

where $D = 4 n_i^2 b - \Delta n_L^2 (b+1)^2$

The arc tan term above takes a log form when D is negative (see Appendix III).

A P P E N D I X V

Added Carrier Densities with Uniform Illumination

A homogeneous n-type semiconductor is uniformly illuminated between the points a and -a. If the time derivatives are zero and one dimensional geometry is assumed, the continuity equation for holes is

$$D_a \frac{d^2 p}{dx^2} + g - r = 0$$

where g and r are the rates per unit volume of carrier generation and recombination. Carrier diffusion will be ambipolar under the above conditions; but if the total hole density is small compared to the total electron density, the ambipolar diffusivity, D_a, is approximately equal to D_p, the hole diffusivity. Assuming a uniform rate, G, of carrier pairs are photo generated per unit volume, the generation and recombination rates are

$$g = \frac{p_o}{\tau_p} \qquad (x > a \quad and \quad x < -a)$$

$$g = \frac{p_o}{\tau_p} + G \qquad (-a < x < a)$$

$$r = \frac{p_o + \Delta n(x)}{\tau_p} \qquad (for \ all \ x)$$

where τ_p is the hole lifetime and $\Delta n(x) = \Delta p(x)$ is the added carrier pair density.

For $X > a$ and $X < -a$ the continuity equation becomes

$$\frac{d^2 \Delta n(x)}{dx^2} - \frac{\Delta n(x)}{D_p \tau_p} = 0$$

Using the boundary conditions

$$\Delta n = 0 \qquad x = \pm \infty$$

$$\Delta n = \Delta n(a) \qquad x = \pm a$$

the solutions of this equation are

$$\Delta n(x) = \Delta n(a) \exp \frac{a-x}{L_p} \qquad (x > a)$$

$$\Delta n(x) = \Delta n(a) \exp \frac{a+x}{L_p} \qquad (x < -a)$$

where $L_p = \sqrt{D_p \tau_p}$ = hole diffusion length.

In the illuminated region the continuity equation becomes

$$\frac{d^2 \Delta n(x)}{dx^2} - \frac{\Delta n(x)}{D_p \tau_p} + \frac{G}{D_p} = 0$$

and

$$\Delta n(x) = G\tau_p + C_1 \exp\left(-\frac{x}{L_p}\right) + C_2 \exp\left(\frac{x}{L_p}\right)$$

The added carrier density $\Delta n(x)$ and its derivative must be continuous at the edges of the illuminated region $X = \pm a$, and from these conditions

$$C_1 = C_2 = C$$

and

$$\Delta n(a) = G\tau_p + 2C \cosh\left(\frac{a}{L_p}\right)$$

Substituting for $\Delta n(a)$

$$C = -G\tau_p \exp\left(-\frac{a}{L_p}\right)$$

and $\quad \Delta n(x) = G \tau_p \left[1 - \exp\left(-\frac{a}{L_p}\right) \cosh\left(\frac{x}{L_p}\right) \right] \qquad (-a < x < a)$

$$\Delta n(x) = \frac{G \tau_p}{2} \left[1 - \exp\left(-\frac{2a}{L_p}\right) \right] \exp\left(\frac{a-x}{L_p}\right) \qquad (x > a)$$

$$\Delta n(x) = \frac{G \tau_p}{2} \left[1 - \exp\left(-\frac{2a}{L_p}\right) \right] \exp\frac{a+x}{L_p} \qquad (x < -a)$$

The ratio

$$\frac{\Delta n(a)}{\Delta n(o)} = \frac{1}{2} \left[1 + \exp\left(-\frac{a}{L_p}\right) \right]$$

shows that the added carrier concentrations at the edges of the illuminated region are always greater than one half the concentration at the mid point.

A P P E N D I X   VI

Added Carrier Concentrations at Illuminated Junctions

When the differences of imrefs at the edges of
a junction transition layer are equal, i.e., when

$$\left(\phi_p - \phi_n\right)_n = \left(\phi_p - \phi_n\right)_p$$

then

$$\frac{p_{op} + (\Delta n_L)_p}{p_{on} + (\Delta n_L)_n} \frac{n_{op} + (\Delta n_L)_p}{n_{on} + (\Delta n_L)_n} = 1$$

Assuming $n_{on} \gg p_{on}$ and $p_{op} \gg n_{op}$ this simplifies
to

$$(\Delta n_L)_p \, p_{op} \left[1 + \frac{(\Delta n_L)_p}{p_{op}}\right] = (\Delta n_L)_n \, n_{on} \left[1 + \frac{(\Delta n_L)_n}{n_{on}}\right]$$

Then for weak illumination, when the added carrier densities
are negligible compared with the majority carrier densities

$$\frac{(\Delta n_L)_p}{(\Delta n_L)_n} = \frac{n_{on}}{p_{op}}$$

and for strong illumination, when the added carrier densities
are large compared with the majority carrier densities

$$(\Delta n_L)_n = (\Delta n_L)_p$$

Similar relations apply to junctions in which one
side is intrinsic and to low-high (L - H) junctions where
there is a large abrupt increase of impurity density. In the
i -n junction

$$\frac{(\Delta n_L)_i}{(\Delta n_L)_n} = \frac{n_{on}}{2 n_i} \qquad\qquad \text{(weak illumination)}$$

and

$$\left(\Delta n_L\right)_i = \left(\Delta n_L\right)_n \qquad \text{(strong illumination)}$$

In the n - n + junction

$$\frac{\left(\Delta n_L\right)_n}{\left(\Delta n_L\right)_{n+}} = \frac{n_{on+}}{n_{on}} \qquad \text{(weak illumination)}$$

$$\left(\Delta n_L\right)_n = \left(\Delta n_L\right)_{n+} \qquad \text{(strong illumination)}$$

BIBLIOGRAPHY

Borneman, E.H., Schwarz, R.F., Steckler, J.J., Rectification Properties of Metal-Semiconductor Contacts, Journal of Applied Physics, 26, 1021 (1955).

Chynoweth, A.G., and Pearson, G.L., Effect of Dislocations on Breakdown in Silicon p-n Junctions, Journal of Applied Physics, 29, 1103 (1958).

Cummerow, R.L., Photovoltaic Effect in p-n Junctions, Physical Review, 95, 16 (1954).

Fan, H.Y., Theory of Photovoltaic Effect of p-n Barrier in Semiconductor, Physical Review, 75, 1631 (1949).

Fink, C.G., Dokras, V.M., Electrodeposition of Germanium, Transactions of Electro-chemical Society, 95, 80 (1949).

Fletcher, N.H., General Semiconductor Junction Relations, Journal of Electronics, 2, 609 (1957).

Frank, H., Photo-electric Measurement of Inner Electric Fields in Inhomogeneous Semiconductors, Czechoslovakian Journal of Physics, 5, 433 (1956).

Gunn, J.B., On Carrier Accumulation, and the Properties of Certain Semiconductor Junctions, Journal of Electronics and Control, 4, 17 (1958).

Misawa, T., Emitter Efficiency of Junction Transistor, Journal of the Physical Society of Japan, 10, 362 (1955).

Morin, F.J., Maita, J.P., Conductivity and Hall Effect in the Intrinsic Range of Germanium, Physical Review, 94, 1525 (1954).

Pearson, G.L., and Bardeen, J., Electrical Properties of Pure Silicon Alloys Containing Boron and Phosphorus, Physical Review, 75, 865 (1949).

Read, W.T., Scattering of Electrons by Charged Dislocations in Semiconductors, Philosophical Magazine, 46, 111 (1955).

Read, W.T., Statistics of the Occupation of Dislocation Acceptor Centers, Philosophical Magazine, 45, 1119 (1954).

Read, W.T., Theory of Dislocations in Germanium,
        Philosophical Magazine, 45, 775 (1954).

Rittner, E.S., Electron Processes in Semiconductors,
        Photoconductivity Conference Atlantic City, John
        Wiley and Sons Incorporated, 1954.

Shockley, W., Electrons and Holes in Semiconductors,
        D. Van Nostrand Company, 1950.

Shockley, W., The Theory of p-n Junctions in Semiconductors
        and p-n Junction Transistors,
        Bell System Technical Journal, 28, 435 (1949).

Stevenson, D.T., Keyes, R.J., Measurements of Carrier
        Lifetimes in Germanium and Silicon,
        Journal of Applied Physics, 26, 190 (1955).

Tauc, J., Generation of an e.m.f. in Semiconductors with Non-
        equilibrium Current Carrier Concentrations,
        Review of Modern Physics, 29, 308 (1957).

Tauc, J., The Theory of a Bulk Photovoltaic Phenomenon in
        Semiconductors,
        Czechoslovakian Journal of Physics, 5, 178 (1955).

Weisberg, A.H., Heavy Rhodium Electroplates Now Possible,
        Materials and Methods, 37, Number 3, 85 (1953).